

**Charmonium production in hot magnetized hyperonic matter  
– effects of baryonic Dirac sea and pseudoscalar-vector meson  
mixing**

Amruta Mishra\*

*Department of Physics, Indian Institute of Technology Delhi,  
Hauz Khas New Delhi 110016 India*

Arvind Kumar<sup>†</sup>

*Department of Physics, Dr. B. R. Ambedkar National  
Institute of Technology Jalandhar, Punjab 144008 India*

S.P. Misra<sup>‡</sup>

*Institute of Physics, Bhubaneswar – 751005, India*

## Abstract

We investigate the medium modifications of the masses of pseudoscalar open charm ( $D$  and  $\bar{D}$ ) mesons and the charmonium state ( $\psi(3770)$ ) in hot isospin asymmetric strange hadronic medium in the presence of an external magnetic field within a chiral effective model. The in-medium partial decay widths of  $\psi(3770)$  to charged and neutral  $D\bar{D}$  mesons are computed from the medium modifications of the masses of the initial and final state mesons. These are computed using two light quark pair creation models - (I) the  $^3P_0$  model and (II) a field theoretical (FT) model of composite hadrons with quark (and antiquark) constituents. The production cross-sections of  $\psi(3770)$ , arising from scattering of the  $D$  and  $\bar{D}$  mesons, are computed from the relativistic Breit-Wigner spectral function expressed in terms of the in-medium masses and the decay widths of the charmonium state. The effects of the magnetic field are considered due to the Dirac sea (DS) of the baryons, the mixing of the pseudoscalar ( $S=0$ ) and vector ( $S=1$ ) meson (PV mixing), the Landau level contributions for the charged hadrons. The anomalous magnetic moments (AMMs) of the baryons are also taken into account in the present study. For magnetized nuclear matter, at  $\rho_B = \rho_0$ , the effect of Dirac sea leads to inverse magnetic catalysis (IMC), which is drop of the magnitude of the light quark condensates (proportional to the scalar fields) with increase in the magnetic field, contrary to the opposite effect of magnetic catalysis (MC) at  $\rho_B = 0$ . The inclusion of hyperons to the nuclear medium is observed to lead to magnetic catalysis. There are observed to be significant effects from the DS and PV mixing on the properties of the charm mesons. The production cross-sections of  $\psi(3770)$  arising due to scattering of  $D^+D^-(D^0\bar{D}^0)$  mesons in the hot magnetized strange hadronic matter are observed to have distinct peak positions, when the magnetic field is large. This is because the production cross-sections have contributions from the transverse as well as longitudinal components of  $\psi(3770)$ , which have non-degenerate masses due to PV ( $\psi(3770) - \eta'_c$ ) mixing. These can have observable consequences on the dilepton spectra as well as on the production of the charm mesons in ultra-relativistic peripheral heavy ion collision experiments, where the produced magnetic field is huge.

---

\*Electronic address: amruta@physics.iitd.ac.in

†Electronic address: kumara@nitj.ac.in

‡Electronic address: misrasibaprasad@gmail.com

## I. INTRODUCTION

Probing the properties of hadrons at finite density and/or temperature is an important and challenging topic of research as it can have implications in understanding the experimental observables from heavy-ion collision experiments as well as has relevance in the physics of compact objects [1, 2]. It has been estimated that magnetic fields of the order of  $2m_\pi^2$  in relativistic heavy-ion collider (RHIC) at BNL, USA and of around  $15m_\pi^2$  in large hadron collider (LHC) at CERN can be produced in non-central heavy-ion collisions, which has initiated lots of studies on the in-medium properties of hadrons under strong magnetic field background [3–5]. Strong magnetic fields are also expected to exist in the dense astrophysical objects, e.g, the magnetars [6–8] and also play an important role in the physics of early universe [1, 2].

The presence of intense magnetic field leads to many interesting physical phenomenon such as magnetic catalysis (MC), inverse magnetic catalysis (IMC), chiral magnetic effect (CME), chiral magnetic wave [9–13]. The time evolution of magnetic field produced in heavy-ion collisions is however still debatable. The strength of magnetic field may decay rapidly in vacuum, but the strongly interacting medium may cause a delay in the decay and hence an increase in the life-time of magnetic field. As discussed in Ref. [13], the decay time of the magnetic field in the medium may increase due to conducting medium formed by charged particles and hence induction effects [14]. The strong magnetic field produced during the initial stages of heavy-ion collisions can have imprints on the experimental observables related to hadrons composed of heavy quarks as these are also produced during that stage, for example, the splitting of the directed flow  $v_1$  of  $D$  and  $\bar{D}$  mesons [15].

The properties of light and heavy meson are studied in the external magnetic field at zero temperature and zero baryonic density [16–19]. The non-perturbative methods such as relativistic mean field (RMF) models [20–23], Nambu Jona Lasinio (NJL) [24] and their polyakov extended versions (PNJL) [25, 26], quark meson coupling model [27], chiral hadronic model [28], chiral quark mean field model [29, 30], QCD sum rule approach, confined isospin density dependent model [31] etc., have been used in the literature to investigate the impact of external magnetic field on the quark matter, nuclear matter and compact star properties. The importance of magnetized Dirac sea in the calculations of the properties of magnetized matter and its role in observation of (inverse) magnetic catalysis effect have been explored

in Refs. [32–34]. In Ref. [33], the vacuum to nuclear matter phase transition was studied using Walecka model as well as an extended linear sigma model, considering Dirac sea of nucleons but neglecting the anomalous magnetic moments of the nucleons. The phenomenon of magnetic catalysis, i.e., the enhancement of chiral condensates with increasing magnetic field, was observed in this work [33]. In Ref. [34], the effects of Dirac sea of nucleons on the vacuum to nuclear matter phase transition were studied within the Walecka model considering finite anomalous magnetic moments of nucleons, and, using the weak magnetic field approximation for computing the nucleon self energy by summation of tadpole diagrams. The anomalous magnetic moments (AMMs) of nucleons were observed to play a crucial role. The magnetic catalysis effect was observed at zero temperature and zero baryon density with as well as without consideration of AMMs. However, at finite temperature and baryonic density, the inverse magnetic catalysis was observed in the presence of AMMs of the nucleons, which was observed to be magnetic catalysis when the AMMs were ignored. The impact of Dirac sea on the properties of nuclear matter using quantum hadrodynamics (QHD) model and performing calculations using covariant propagators [35] for the nucleons with complete effect of magnetic field and anomalous magnetic moments of nucleons has been investigated in Ref. [36]. The phenomenon of inverse magnetic catalysis was also reported in some lattice QCD calculations [11], where the critical temperature,  $T_c$  was observed to decrease with increase in the magnetic field. The effects of the Dirac sea for quark matter were investigated using NJL model in [24, 32]. The phenomenon of inverse magnetic catalysis was observed in a study of magnetic effects on chiral phase transition in a modified AdS/QCD model [37, 38].

The properties of heavy flavour mesons at finite density and temperature, have been explored extensively in the past, both for zero as well as finite magnetic field background. In Refs. [39, 40], the properties of pseudoscalar  $D$  and  $\bar{D}$  mesons were studied in nuclear matter at finite temperatures within a chiral SU(3) model [41], generalized to SU(4) sector to include the interactions of the charmed mesons. The properties of open charmed mesons and charmonium states have been studied in strange hadronic matter in Refs. [42, 43]. The chiral SU(3) model has also been generalized to SU(5) sector to study the properties of bottom mesons in nuclear and strange hadronic matter [44–46]. The chiral model has also been extended to study the impact of strong magnetic field on open charm mesons, open bottom mesons, charmonium and bottomonium properties in nuclear medium in Refs.

[47–51]. The conjunction of chiral SU(3) model and QCD sum rule approach has also been used to study the properties of open and hidden heavy mesons at finite density and temperature for nonzero magnetic field [52–55]. In the presence of finite strong magnetic field the phenomenon of PV mixing which accounts for the interaction of pseudoscalar mesons with the longitudinal component of vector mesons has been studied in context of heavy flavored mesons in Refs. [56–58]. Recently, chiral SU(3) model is generalized to explore the impact of magnetized Dirac sea on the in-medium properties of different mesons [59–63]. Within effective SU(4) model the properties of charmed mesons were studied in the nuclear matter at zero temperature, in the presence of strong external magnetic field including the impact of Dirac sea [63]. The magnetized Dirac sea along with finite anomalous magnetic moment of nucleons is observed to lead to the phenomenon of inverse magnetic catalysis at finite densities for symmetric as well as asymmetric nuclear matter in presence of strong magnetic fields. The effects of the magnetized Dirac sea on the spectral properties of light vector and axial-vector mesons in hot magnetized nuclear matter have also been studied recently using a QCD sum rule approach in Ref. [64].

In peripheral ultra-relativistic heavy ion collision experiments (where strong magnetic fields are created), since the matter produced is extremely dilute, we study the decay width of the charmonium state  $\psi(3770)$ , which is the lowest state which decays to  $D\bar{D}$  in vacuum. In the present work, we investigate the in-medium masses of pseudoscalar  $D$  and  $\bar{D}$  mesons and charmonium state  $\psi(3770)$  and their effect on the partial decay width of  $\psi(3770) \rightarrow D\bar{D}$  in isospin asymmetric strange hadronic matter at finite temperatures in presence of a strong magnetic field. The effects of the magnetized baryon Dirac sea contributions as well as the PV mixing (the mixing of the pseudoscalar meson (S=0) and the longitudinal component of the vector meson (S=1)) on the masses of the charmed mesons are taken into consideration. The influence of magnetized Dirac sea of nucleons ( $p, n$ ) and hyperons ( $\Lambda, \Sigma^{\pm,0}, \Xi^{-,0}$ ) on the meson masses are explored, accounting for the finite anomalous magnetic moments (AMMs) of the baryons. Additionally, the lowest Landau level contributions are considered for the charged open charm mesons. The decay width of heavy quarkonium state to open heavy flavour mesons, arising due to the mass modifications of the initial and final state mesons, are computed using (I) the  $^3P_0$  model [65, 66] for the charm sector, as well as (II) a field theoretical (FT) model of composite hadrons with quark (and antiquark) constituents for both charm and bottom sectors [57, 62, 67–70]. In both of these models, the charmonium

decay proceeds through creation of a light quark-antiquark pair and the heavy charm quark (antiquark) combines with the light antiquark (quark) to form  $D\bar{D}$  in the final state. The impact of PV mixing on the in-medium properties of open charm and charmonium states are observed to be quite significant in the present work. The well-separated non-degenerate masses of the longitudinal and transverse components of  $\psi(3770)$  due to PV mixing is observed to be at distinct peak positions in the production cross-sections of  $\psi(3770)$  due to scattering of the  $D^+D^-(D^0\bar{D}^0)$  mesons, when the magnetic field is large.

Following is the outline of this paper: in section II we give a brief description of the chiral effective model used to calculate the masses of the charmed mesons in the finite temperature magnetized matter at zero density as well as for isospin asymmetric (strange) hadronic matter. In section III, the procedure to calculate the in-medium masses of  $D$ ,  $\bar{D}$  and the charmonium  $\psi(3770)$  and the medium modifications of the decay width of  $\psi(3770) \rightarrow D\bar{D}$  due to the mass modifications of these mesons is described. The computation of the decay widths using the light quark-antiquark pair creation models – (I) the  $^3P_0$  model and (II) a field theoretical (FT) model of composite hadrons with quark (and antiquark) constituents, are briefly described in this section. The results and discussions of the present study are given in section IV and the work is summarized in section V.

## II. CHIRAL EFFECTIVE MODEL

In this section we briefly describe the chiral effective model used in the present work to study the in-medium properties of charmed mesons at finite temperatures in the presence of an external magnetic field, for zero density as well as in isospin asymmetric (strange) hadronic matter. A chiral SU(3) model incorporating the nonlinear realization of chiral symmetry [41, 71–73] and the broken scale invariance property of QCD [41, 74, 75] is generalized to SU(4) to include the interactions of the charm mesons [39, 42]. The Lagrangian density of chiral SU(3) model is written as [41]

$$\mathcal{L} = \mathcal{L}_{kin} + \sum_{W=X,Y,V,A,u} \mathcal{L}_{BW} + \mathcal{L}_{vec} + \mathcal{L}_0 + \mathcal{L}_{scale\ break} + \mathcal{L}_{SB} + \mathcal{L}_{mag}. \quad (1)$$

In Eq.(1),  $\mathcal{L}_{kin}$  is the kinetic energy term,  $\mathcal{L}_{BW}$  is the baryon-meson interaction term in which the baryons-spin-0 meson interaction term generates the baryon masses.  $\mathcal{L}_{vec}$  describes the dynamical mass generation of the vector mesons via couplings to the scalar mesons and con-

tain additionally quartic self-interactions of the vector fields.  $\mathcal{L}_0$  contains the meson-meson interaction terms,  $\mathcal{L}_{scale\ break}$  is the scale invariance breaking term expressed in terms of logarithmic potential of a dilaton field,  $\mathcal{L}_{SB}$  describes the explicit chiral symmetry breaking. The last term  $\mathcal{L}_{mag}$  describes the interaction of the baryons with the electromagnetic field.

In the present study of isospin asymmetric strange hadronic matter at finite magnetic field, we adopt the mean field approximation, in which the meson fields are replaced by their expectation values. The meson fields which have non-zero expectation values are the scalar  $(\sigma, \zeta, \delta)$  and the vector fields,  $\omega^\mu \rightarrow \omega\delta^{\mu 0}$ ,  $\rho^{\mu a} \rightarrow \rho\delta^{\mu 0}\delta_{a3}$  and,  $\phi^\mu \rightarrow \phi\delta^{\mu 0}$ , and, the expectation values of the other mesons are zero. We also use the approximations  $\bar{\psi}_i\psi_j \rightarrow \delta_{ij}\langle\bar{\psi}_i\psi_i\rangle \equiv \delta_{ij}\rho_s^i$  and  $\bar{\psi}_i\gamma^\mu\psi_j \rightarrow \delta_{ij}\delta^{\mu 0}\langle\bar{\psi}_i\gamma^0\psi_i\rangle \equiv \delta_{ij}\delta^{\mu 0}\rho_i$ , where,  $\rho_s^i$  and  $\rho_i$  are the scalar and number density of baryon of species,  $i$ . In the above approximation, the terms which contribute to the baryon-meson interaction,  $\mathcal{L}_{BW}$  of equation (1) arise from the interactions due to the scalar (S) and the vector (V) mesons, and, is given as

$$\mathcal{L}_{BS} + \mathcal{L}_{BV} = \sum_i \bar{\psi}^i (g_{\sigma i}\sigma + g_{\zeta i}\zeta + g_{\delta i}\delta - g_{\omega i}\gamma^0\omega - g_{\rho i}\gamma^0\rho - g_{\phi i}\gamma^0\phi)\psi^i. \quad (2)$$

The effective mass of the baryon of species  $i$  is obtained from the in-medium values of the scalar-isoscalar non-strange ( $\sigma$ ) and strange ( $\zeta$ ) mesons and the scalar-isovector ( $\delta$ ) meson and is given as

$$m_i^* = -g_{\sigma i}\sigma - g_{\zeta i}\zeta - g_{\delta i}\delta, \quad (3)$$

and the effective chemical potential for  $i$ -th baryon, due to the interaction with the vector mesons ( $\omega$ ,  $\rho$  and  $\phi$ ) is given as

$$\mu_i^* = \mu_i - g_{\omega i}\omega - g_{\rho i}\rho - g_{\phi i}\phi \quad (4)$$

The other terms in the Lagrangian density of equation (1) are given as

$$\mathcal{L}_{vec} = \frac{1}{2}\frac{\chi^2}{\chi_0^2}\left(m_\omega^2\omega^2 + m_\rho^2\rho^2 + m_\phi^2\phi^2\right) + g_4^4(\omega^4 + 2\phi^4 + 6\omega^2\rho^2 + \rho^4) \quad (5)$$

$$\begin{aligned} \mathcal{L}_0 = & -\frac{1}{2}k_0\chi^2(\sigma^2 + \zeta^2 + \delta^2) + k_1(\sigma^2 + \zeta^2 + \delta^2)^2 \\ & + k_2\left(\frac{\sigma^4}{2} + \frac{\delta^4}{2} + \zeta^4 + 3\sigma^2\delta^2\right) + k_3\chi(\sigma^2 - \delta^2)\zeta - k_4\chi^4 \end{aligned} \quad (6)$$

$$\mathcal{L}_{scale\ break} = -\frac{1}{4}\chi^4\ln\frac{\chi^4}{\chi_0^4} + \frac{d}{3}\chi^4\ln\left(\frac{(\sigma^2 - \delta^2)\zeta}{\sigma_0^2\zeta_0}\left(\frac{\chi}{\chi_0}\right)^3\right), \quad (7)$$

$$\mathcal{L}_{SB} = -\left(\frac{\chi}{\chi_0}\right)^2\left[m_\pi^2 f_\pi\sigma + \left(\sqrt{2}m_K^2 f_K - \frac{1}{\sqrt{2}}m_\pi^2 f_\pi\right)\zeta\right], \quad (8)$$

and,

$$\mathcal{L}_{mag} = -\bar{\psi}_i q_i \gamma_\mu A^\mu \psi_i - \frac{1}{2} \kappa_i \bar{\psi}_i \sigma^{\mu\nu} F_{\mu\nu} \psi_i - \frac{1}{4} F^{\mu\nu} F_{\mu\nu}. \quad (9)$$

In the above, the parameters  $k_0$ ,  $k_2$  and  $k_4$  are fitted to ensure extremum in the vacuum for the equations of motion for scalar fields  $\sigma$ ,  $\zeta$  and the dilaton field  $\chi$ ,  $k_1$  is fitted to reproduce the mass of  $\sigma$  to be of the order of 500 MeV,  $k_3$  is fitted from the  $\eta$  and  $\eta'$  masses, and the value of the  $\chi$  in vacuum is fitted so that the pressure  $p = 0$  at the nuclear matter saturation density. In equation (9),  $q_i$  is the electric charge of the  $i^{\text{th}}$  baryon described by field  $\psi_i$ . The second term is a tensorial interaction term expressed in terms of the electromagnetic field tensor,  $F_{\mu\nu} (= \partial_\mu A_\nu - \partial_\nu A_\mu)$ ,  $\sigma^{\mu\nu} = \frac{i}{2}[\gamma^\mu, \gamma^\nu]$ , and  $\kappa_i$ , the anomalous magnetic moment (AMM) of  $i$ -th baryon.

The concept of broken scale invariance leading to the trace anomaly in QCD,  $\theta_\mu^\mu = \frac{\beta_{QCD}}{2g} G_{\mu\nu}^a G^{\mu\nu a}$ , where  $G_{\mu\nu}^a$  is the gluon field strength tensor of QCD, is simulated in the effective Lagrangian at tree level through the introduction of the scale breaking term [76, 77] given by equation (8). Equating the trace of the energy momentum tensor with that of the present chiral model gives the relation of the dilaton field to the scalar gluon condensate. The explicit symmetry breaking term in the chiral model is given by

$$\mathcal{L}_{SB} = - \left( \frac{\chi}{\chi_0} \right)^2 \text{Tr} \left[ \text{diag} \left( \frac{m_\pi^2 f_\pi}{2} (\sigma + \delta), \frac{m_\pi^2 f_\pi}{2} (\sigma - \delta), \left( \sqrt{2} m_K^2 f_K - \frac{1}{\sqrt{2}} m_\pi^2 f_\pi \right) \zeta \right) \right] \quad (10)$$

which reduces to eqn. (8), and in QCD, this term is given as  $\mathcal{L}_{SB}^{QCD} = -\text{Tr}[\text{diag}(m_u \bar{u}u, m_d \bar{d}d, m_s \bar{s}s)]$ . In the above, the matrices, whose traces give the corresponding Lagrangian densities have been explicitly written down, and a comparison of their matrix elements relates the quark condensates to the values of the scalar fields as given by [78]

$$\begin{aligned} m_u \langle \bar{u}u \rangle &= \left( \frac{\chi}{\chi_0} \right)^2 \frac{m_\pi^2 f_\pi}{2} (\sigma + \delta), \quad m_d \langle \bar{d}d \rangle = \left( \frac{\chi}{\chi_0} \right)^2 \frac{m_\pi^2 f_\pi}{2} (\sigma - \delta), \\ m_s \langle \bar{s}s \rangle &= \left( \frac{\chi}{\chi_0} \right)^2 \left( \sqrt{2} m_K^2 f_K - \frac{1}{\sqrt{2}} m_\pi^2 f_\pi \right) \zeta. \end{aligned} \quad (11)$$

The thermodynamic potential for the magnetized hadronic medium is written as

$$\Omega = \Omega_{DS} + \Omega_{med} - \mathcal{L}_{vec} - \mathcal{L}_0 - \mathcal{L}_{scale\ break} - \mathcal{L}_{SB}. \quad (12)$$

In the equation (12),  $\Omega_{DS}$  and  $\Omega_{med}$  denote the contributions of Dirac sea (DS) and Fermi sea (medium part) of the (charged and neutral) baryons to the thermodynamic potential,



with the masses and chemical potentials of the baryons, modified due to their interactions with the scalar and vector fields, given by equations (3) and (4) respectively. For spin-1/2 charged baryons ( $i = p, \Sigma^\pm, \Xi^-$ ), these are given as [33, 35, 36]

$$\Omega_{\text{DS}}^{\text{charged}} = \sum_i \Omega_{\text{DS}}^i = - \sum_i \frac{|q_i B|}{2\pi} \sum_{s=\pm 1} \sum_{\nu=0}^{\infty} (2 - \delta_{\nu 0}) \int_{-\infty}^{\infty} \frac{dk_z}{2\pi} \epsilon_{k,\nu,s}^i, \quad (13)$$

and

$$\Omega_{\text{med}}^{\text{charged}} = \sum_i \Omega_{\text{med}}^i = -T \sum_i \frac{|q_i B|}{2\pi} \sum_{s=\pm 1} \sum_{\nu=0}^{\infty} (2 - \delta_{\nu 0}) \int_{-\infty}^{\infty} \frac{dk_z}{2\pi} \left\{ \ln \left( 1 + e^{-\beta(\epsilon_{k,\nu,s}^i - \mu_i^*)} \right) + \ln \left( 1 + e^{-\beta(\epsilon_{k,\nu,s}^i + \mu_i^*)} \right) \right\}, \quad (14)$$

where, where  $\beta = 1/T$  and  $\epsilon_{k,\nu,s}^i$  is the single particle energy of the  $i$ -th charged baryon given as

$$\epsilon_{k,\nu,s}^i = \sqrt{k_z^2 + \left( \sqrt{2\nu|q_i B| + m_i^{*2}} - s\kappa_i B \right)^2}. \quad (15)$$

The thermodynamic potentials corresponding to the Dirac sea and the Fermi sea of the neutral baryons ( $i = n, \Lambda, \Sigma^0, \Xi^0$ ) are given as [33, 35, 36]

$$\Omega_{\text{DS}}^{\text{Neutral}} = \sum_i \Omega_{\text{DS}}^i = - \sum_i \sum_{s=\pm 1} \int \frac{d^3 k}{(2\pi)^3} \epsilon_{k,s}^i, \quad (16)$$

and,

$$\Omega_{\text{med}}^{\text{Neutral}} = \sum_i \Omega_{\text{med}}^i = -T \sum_i \sum_{s=\pm 1} \int \frac{d^3 k}{(2\pi)^3} \left\{ \ln \left( 1 + e^{-\beta(\epsilon_{k,s}^i - \mu_i^*)} \right) + \ln \left( 1 + e^{-\beta(\epsilon_{k,s}^i + \mu_i^*)} \right) \right\}, \quad (17)$$

with the single particle energy for the  $i$ -th neutral baryon given as

$$\epsilon_{k,s}^i = \sqrt{k_z^2 + \left( \sqrt{k_x^2 + k_y^2 + m_i^{*2}} - s\kappa_i B \right)^2}. \quad (18)$$

For given values of the baryon density,  $\rho_B = \sum_i \rho_i$ , with  $\rho_i$  as the number density of the  $i$ -th baryon, the isospin asymmetry parameter  $\eta = -\frac{\Sigma_i I_{3i} \rho_i}{\rho_B}$ , with  $I_{3i}$  as the 3<sup>rd</sup> component of isospin quantum number of the  $i$ -th baryon, the strangeness fraction,  $f_s = \frac{\Sigma_i |s_i| \rho_i}{\rho_B}$ , with  $s_i$  number of strange quarks in the  $i$ -th baryon, temperature,  $T$  and magnetic field,  $B$ , the minimisation of the thermodynamic potential leads to the coupled equations for the scalar fields ( $\sigma, \zeta, \delta$ ), the dilaton field  $\chi$ , and the vector fields ( $\omega, \rho, \phi$ ) as given by

$$\begin{aligned} & k_0 \chi^2 \sigma - 4k_1 (\sigma^2 + \zeta^2 + \delta^2) \sigma - 2k_2 (\sigma^3 + 3\sigma\delta^2) - 2k_3 \chi \sigma \zeta \\ & - \frac{d}{3} \chi^4 \left( \frac{2\sigma}{\sigma^2 - \delta^2} \right) + \left( \frac{\chi}{\chi_0} \right)^2 m_\pi^2 f_\pi - \sum_i g_{\sigma i} \rho_s^i = 0 \end{aligned} \quad (19)$$

$$\begin{aligned}
& k_0\chi^2\zeta - 4k_1(\sigma^2 + \zeta^2 + \delta^2)\zeta - 4k_2\zeta^3 - k_3\chi(\sigma^2 - \delta^2) \\
& - \frac{d\chi^4}{3\zeta} + \left(\frac{\chi}{\chi_0}\right)^2 \left[ \sqrt{2}m_K^2 f_K - \frac{1}{\sqrt{2}}m_\pi^2 f_\pi \right] - \sum_i g_{\zeta i} \rho_s^i = 0
\end{aligned} \tag{20}$$

$$\begin{aligned}
& k_0\chi^2\delta - 4k_1(\sigma^2 + \zeta^2 + \delta^2)\delta - 2k_2(\delta^3 + 3\sigma^2\delta) + k_3\chi\delta\zeta \\
& + \frac{2}{3}d\left(\frac{\delta}{\sigma^2 - \delta^2}\right) - \sum_i g_{\delta i} \rho_s^i = 0
\end{aligned} \tag{21}$$

$$\begin{aligned}
& k_0\chi(\sigma^2 + \zeta^2 + \delta^2) - k_3(\sigma^2 - \delta^2)\zeta + \chi^3 \left[ 1 + \ln\left(\frac{\chi^4}{\chi_0^4}\right) \right] + (4k_4 - d)\chi^3 \\
& - \frac{4}{3}d\chi^3 \ln\left(\left(\frac{(\sigma^2 - \delta^2)\zeta}{\sigma_0^2\zeta_0}\right)\left(\frac{\chi}{\chi_0}\right)^3\right) + \frac{2\chi}{\chi_0^2} \left[ m_\pi^2 f_\pi \sigma + \left( \sqrt{2}m_K^2 f_K - \frac{1}{\sqrt{2}}m_\pi^2 f_\pi \right) \zeta \right] = 0
\end{aligned} \tag{22}$$

$$\left(\frac{\chi}{\chi_0}\right)^2 m_\omega^2 \omega + g_4^4 (4\omega^3 + 12\rho^2 \omega) - \sum_i g_{\omega i} \rho_i = 0, \tag{23}$$

$$\left(\frac{\chi}{\chi_0}\right)^2 m_\rho^2 \rho + g_4^4 (4\rho^3 + 12\omega^2 \rho) - \sum_i g_{\rho i} \rho_i = 0, \tag{24}$$

$$\left(\frac{\chi}{\chi_0}\right)^2 m_\phi^2 \phi + 8g_4^4 \phi^3 - \sum_i g_{\phi i} \rho_i = 0, \tag{25}$$

where,  $\rho_i$  is the number density of the  $i$ -th baryon, given by the expression

$$\rho_i = \frac{|q_i B|}{2\pi^2} \sum_{s=\pm 1} \sum_{\nu=0}^{\infty} (2 - \delta_{\nu 0}) \int_0^\infty dk_z \left[ \frac{1}{1 + e^{\beta(\epsilon_{k,\nu,s}^i - \mu_i^*)}} - \frac{1}{1 + e^{\beta(\epsilon_{k,\nu,s}^i + \mu_i^*)}} \right], \tag{26}$$

for charged baryons and

$$\rho_i = \sum_{s=\pm 1} \int \frac{d^3 k}{(2\pi)^3} \left[ \frac{1}{1 + e^{\beta(\epsilon_{k,s}^i - \mu_i^*)}} - \frac{1}{1 + e^{\beta(\epsilon_{k,s}^i + \mu_i^*)}} \right], \tag{27}$$

for the neutral baryons. In the above equations, the scalar density of the  $i$ -th baryon,  $\rho_s^i = \langle \bar{\psi}^i \psi^i \rangle = \partial\Omega/\partial m_i^*$ . The expectation values of the scalar fields ( $\sigma$ ,  $\zeta$  and  $\delta$ ) are obtained by solving the equations self-consistently, since these values depend on the baryon scalar densities,  $\rho_s^i$ , which, in turn, are functions of the scalar field (through the effective baryon

masses). Neglecting the contribution from the Dirac sea to the thermodynamic potential, the expression for the scalar density of the  $i$ -th baryon,  $\rho_s^i$  is given as

$$\rho_s^i \equiv \rho_s^{i\text{med}} = \frac{|q_i|B}{2\pi^2} \sum_{s=\pm 1} \sum_{\nu=0}^{\infty} (2 - \delta_{\nu 0}) m_i^* \int_0^{\infty} dk_z \frac{\sqrt{m_i^{*2} + 2\nu|q_i|B - s\kappa_i B}}{\epsilon_{k,\nu,s}^i \sqrt{m_i^{*2} + 2\nu|q_i|B}} \times \left[ \frac{1}{1 + e^{\beta(\epsilon_{k,\nu,s}^i - \mu_i^*)}} + \frac{1}{1 + e^{\beta(\epsilon_{k,\nu,s}^i + \mu_i^*)}} \right], \quad (28)$$

for the charged baryons and

$$\rho_s^i \equiv \rho_s^{i\text{med}} = m_i^* \int \frac{d^3k}{(2\pi)^3} \sum_{s=\pm 1} \frac{\sqrt{k_x^2 + k_y^2 + m_i^{*2} - s\kappa_i B}}{\epsilon_{k,s}^i \sqrt{k_x^2 + k_y^2 + m_i^{*2}}} \left[ \frac{1}{1 + e^{\beta(\epsilon_{k,s}^i - \mu_i^*)}} + \frac{1}{1 + e^{\beta(\epsilon_{k,s}^i + \mu_i^*)}} \right], \quad (29)$$

for the neutral baryons. Within the chiral effective model, the effects of the magnetic field have been studied for isospin asymmetric nuclear matter on the open charm [47], open bottom [48], charmonium [49] and bottomonium [51] states, considering the effects of the nucleon AMMs. However, these studies were without incorporating the effects of the nucleon Dirac sea, and, were considering only the contributions from the medium parts of the scalar densities for the charged and neutral baryons given by equations (28) and (29), while solving the values of the scalar fields ( $\sigma$ ,  $\zeta$ ,  $\delta$  and  $\chi$ ), along with the vector fields, from the equations (19)-(25). In the present work of the study the charmed mesons in hot strange hadronic matter in the presence of an external magnetic field, the values of the scalar fields are solved including the contributions to the scalar densities from the Dirac sea of baryons. As may be noted, the expressions corresponding to the contributions to the thermodynamic potential from the Dirac sea for the charged and neutral baryons, given by equations (13) and (16) are divergent and need renormalization. In Ref. [33], the nuclear matter in strong magnetic fields was studied within the Walecka model as well as an extended linear sigma model, ignoring the anomalous magnetic moments (AMMs) of the nucleons and the renormalization of the Dirac sea contribution due to the charged baryon, i.e., proton, was carried out by using proper time method. Due to its smallness, the pure vacuum ( $\rho_B=0$ ,  $T=0$ ) contribution corresponding to zero magnetic field was neglected, and the magnetized Dirac sea (the part with non-zero B) was observed to lead to magnetic catalysis. There was no contribution from the neutron due to the Dirac sea, since the AMM of the neutron was not considered. Including the AMMs of the nucleons into account, the covariant fermion propagator in the

presence of strong magnetic fields at finite temperature and density has been calculated in Ref. [35], which has been generalized to include the effects of the Dirac sea in Ref. [36]. The value of the scalar field,  $\sigma$  is calculated through the minimisation of the thermodynamic potential [33], from which the effective mass of the nucleon is obtained. There is observed to be increase in the nucleon mass (corresponding to increase in the light quark condensates) with the increase in the magnetic field, when the AMMs of the nucleons are not considered [33], an effect called the magnetic catalysis (MC). On the other hand, the inclusion of the AMMs is observed to lead to the opposite behaviour for the light quark condensates, i.e., the effect of inverse magnetic catalysis (IMC) [34]. In Ref. [34], the baryon propagator in the presence of a magnetic field was calculated accounting for the AMMs of the nucleons within Walecka model, including the effects of the Dirac sea by summing up the scalar ( $\sigma$ ) and vector ( $\omega$ ) tadpole diagrams in the weak field approximation. In the present study of magnetized hot strange hadronic matter within the chiral effective model, the contribution of the magnetized Dirac sea to the baryon self energy is calculated by summing the scalar ( $\sigma$ ,  $\zeta$  and  $\delta$ ) and vector ( $\omega$ ,  $\rho$  and  $\phi$ ) tadpole diagrams, arising from the baryon-meson interaction given by equation (2) within the weak field approximation. The propagator for the  $i$ -th baryon,  $S_B^i(p)$  is given by [34, 79]

$$\left[ \gamma^\mu p_\mu - \frac{i}{2} q_i F^{\mu\nu} \gamma_\mu \frac{\partial}{\partial p^\nu} - m_i^* - \frac{1}{2} \kappa_i F^{\mu\nu} \sigma_{\mu\nu} \right] S_B^i(p) = 1, \quad (30)$$

where,  $q_i$  and  $\kappa_i$  are the electric charge and AMM of the  $i$ -th baryon,  $m_i^*$  is its effective baryon mass, given by equation (3). The baryon propagator is expanded in powers of  $q_i B$  and  $\kappa_i B$ , retaining upto quadratic order in the weak field approximation. The divergent expression for the self-energy for pure vacuum ( $B=0$ ),  $\Sigma_{DS,B=0}$  is neglected due to its smallness [33, 34]. The dimensional regularization is used to separate the divergent contribution of the magnetized Dirac sea contribution,  $\Sigma_{DS,B}^{div}$ , followed by  $\overline{MS}$  prescription and determination of the scale parameter,  $\Lambda$ , using the condition  $\Sigma_{DS,B}^{div}(m_i^* = m_i) = 0$ . In the present study of magnetized strange hadronic matter at finite temperature, within the chiral effective model, the contribution to the self energy of the  $i$ -th baryon due to the Dirac sea is given as

$$\Sigma^{DS,i} = - \left( \frac{g_{\sigma i}^2}{m_\sigma^2} + \frac{g_{\zeta i}^2}{m_\zeta^2} + \frac{g_{\delta i}^2}{m_\delta^2} \right) \rho_s^{DS,i} \equiv -A_i \rho_s^{DS,i}, \quad (31)$$

where,

$$\rho_s^{DS,i} = -\frac{1}{4\pi^2} \left[ \frac{(q_i B)^2}{3m_i^*} + \{(\kappa_i B)^2 m_i^* + (|q_i| B)(\kappa_i B)\} \left( \frac{1}{2} + 2 \ln \left( \frac{m_i^*}{m_i} \right) \right) \right]. \quad (32)$$

The effects of the Dirac sea of the baryons are taken into consideration by adding the Dirac sea contributions to the scalar densities for the baryons. The contribution from the magnetized Dirac sea to the scalar density of the  $i$ -th baryon, with electric charge,  $q_i$ , the anomalous magnetic moment,  $\kappa_i$  and effective mass,  $m_i^*$ , is given by equation (32). As has already been mentioned, the values of scalar fields  $\sigma$ ,  $\zeta$ ,  $\delta$ , the dilaton field  $\chi$ , along with the vector fields, are obtained by solutions of their coupled equations of motion as given by equations (19)-(25), for given values of the temperature ( $T$ ) and magnetic field ( $B$ ), for zero baryon density, as well as, for (strange) hadronic matter for given values of baryon density ( $\rho_B$ ), isospin asymmetry parameter ( $\eta$ ) and strangeness fraction ( $f_s$ ). These are used to obtain the in-medium masses of the open charm ( $D$  and  $\bar{D}$ ) mesons, the charmonium  $\psi(3770)$ , and the partial decay width of  $\psi(3770) \rightarrow D\bar{D}$  in magnetized isospin asymmetric strange hadronic matter at finite temperatures. The production cross-sections of  $\psi(3770)$  due to the scattering of the charged and neutral  $D\bar{D}$  pairs are obtained using the in-medium masses and the decay widths in the present work.

### III. CHARM MESONS IN HOT ISOSPIN ASYMMETRIC MAGNETIZED STRANGE HADRONIC MATTER

#### A. Masses of open charm and charmonium states

In magnetized isospin asymmetric strange hadronic matter at finite temperatures, the medium modifications of the masses of the open charm ( $D$  and  $\bar{D}$ ) mesons arise due to their interactions with the nucleons, hyperons and the scalar mesons ( $\sigma$  and  $\delta$ ), whereas, the in-medium mass of the charmonium state  $\psi(3770)$  is calculated from the medium change of a dilaton field (which mimics the gluon condensates of QCD) within a chiral effective model

[42]. The interaction Lagrangian density for  $D$  and  $\bar{D}$  mesons is given as [42]

$$\begin{aligned}
\mathcal{L}_{\mathcal{D}(\bar{\mathcal{D}})} = & -\frac{i}{8f_D^2} \left[ 3 \left( \bar{p}\gamma^\mu p + \bar{n}\gamma^\mu n \right) \left( \left( D^0(\partial_\mu \bar{D}^0) - (\partial_\mu D^0)\bar{D}^0 \right) + \left( D^+(\partial_\mu D^-) - (\partial_\mu D^+)D^- \right) \right) \right. \\
& + \left( \bar{p}\gamma^\mu p - \bar{n}\gamma^\mu n \right) \left( \left( D^0(\partial_\mu \bar{D}^0) - (\partial_\mu D^0)\bar{D}^0 \right) - \left( D^+(\partial_\mu D^-) - (\partial_\mu D^+)D^- \right) \right) \\
& + 2 \left( \bar{\Lambda}^0\gamma^\mu \Lambda^0 \right) \left( \left( D^0(\partial_\mu \bar{D}^0) - (\partial_\mu D^0)\bar{D}^0 \right) + \left( D^+(\partial_\mu D^-) - (\partial_\mu D^+)D^- \right) \right) \\
& + 2 \left( \left( \bar{\Sigma}^+\gamma^\mu \Sigma^+ + \bar{\Sigma}^-\gamma^\mu \Sigma^- \right) \left( \left( D^0(\partial_\mu \bar{D}^0) - (\partial_\mu D^0)\bar{D}^0 \right) + \left( D^+(\partial_\mu D^-) - (\partial_\mu D^+)D^- \right) \right) \right) \\
& + \left( \bar{\Sigma}^+\gamma^\mu \Sigma^+ - \bar{\Sigma}^-\gamma^\mu \Sigma^- \right) \left( \left( D^0(\partial_\mu \bar{D}^0) - (\partial_\mu D^0)\bar{D}^0 \right) - \left( D^+(\partial_\mu D^-) - (\partial_\mu D^+)D^- \right) \right) \\
& + 2 \left( \bar{\Sigma}^0\gamma^\mu \Sigma^0 \right) \left( \left( D^0(\partial_\mu \bar{D}^0) - (\partial_\mu D^0)\bar{D}^0 \right) + \left( D^+(\partial_\mu D^-) - (\partial_\mu D^+)D^- \right) \right) \\
& + \left( \bar{\Xi}^0\gamma^\mu \Xi^0 + \bar{\Xi}^-\gamma^\mu \Xi^- \right) \left( \left( D^0(\partial_\mu \bar{D}^0) - (\partial_\mu D^0)\bar{D}^0 \right) + \left( D^+(\partial_\mu D^-) - (\partial_\mu D^+)D^- \right) \right) \\
& + \left. \left( \bar{\Xi}^0\gamma^\mu \Xi^0 - \bar{\Xi}^-\gamma^\mu \Xi^- \right) \left( \left( D^0(\partial_\mu \bar{D}^0) - (\partial_\mu D^0)\bar{D}^0 \right) - \left( D^+(\partial_\mu D^-) - (\partial_\mu D^+)D^- \right) \right) \right] \\
& + \frac{m_D^2}{2f_D} \left[ (\sigma + \sqrt{2}\zeta_c)(\bar{D}^0 D^0 + (D^- D^+)) + \delta((\bar{D}^0 D^0) - (D^- D^+)) \right] \\
& - \frac{1}{f_D} \left[ (\sigma + \sqrt{2}\zeta_c) \left( (\partial_\mu \bar{D}^0)(\partial^\mu D^0) + (\partial_\mu D^-)(\partial^\mu D^+) \right) + \delta \left( (\partial_\mu \bar{D}^0)(\partial^\mu D^0) - (\partial_\mu D^-)(\partial^\mu D^+) \right) \right] \\
& + \frac{d_1}{2f_D^2} (\bar{p}p + \bar{n}n + \bar{\Lambda}^0\Lambda^0 + \bar{\Sigma}^+\Sigma^+ + \bar{\Sigma}^0\Sigma^0 + \bar{\Sigma}^-\Sigma^- + \bar{\Xi}^0\Xi^0 + \bar{\Xi}^-\Xi^-) ((\partial_\mu D^-)(\partial^\mu D^+) \\
& + (\partial_\mu \bar{D}^0)(\partial^\mu D^0)) + \frac{d_2}{2f_D^2} \left[ \left( \bar{p}p + \frac{1}{6}\bar{\Lambda}^0\Lambda^0 + \bar{\Sigma}^+\Sigma^+ + \frac{1}{2}\bar{\Sigma}^0\Sigma^0 \right) (\partial_\mu \bar{D}^0)(\partial^\mu D^0) \right. \\
& \left. + \left( \bar{n}n + \frac{1}{6}\bar{\Lambda}^0\Lambda^0 + \bar{\Sigma}^-\Sigma^- + \frac{1}{2}\bar{\Sigma}^0\Sigma^0 \right) (\partial_\mu D^-)(\partial^\mu D^+) \right], \tag{33}
\end{aligned}$$

where, the first term is the vectorial Weinberg Tomozawa interaction term, the second term is the scalar exchange term, which is obtained from the explicit symmetry breaking term, and, the last three terms ( $\sim (\partial_\mu \bar{D})(\partial^\mu D)$ ) are known as the range terms. The parameters  $d_1$  and  $d_2$  in the range terms are fitted to the empirical values of kaon-nucleon scattering lengths for  $I = 0$  and  $I = 1$  [80, 81]. From the interaction Lagrangian density, using the Fourier transformations of equations of motion, the dispersion relations for  $D$  and  $\bar{D}$  mesons are obtained as

$$-\omega^2 + \vec{k}^2 + m_{D(\bar{D})}^2 - \Pi_{D(\bar{D})}(\omega, |\vec{k}|) = 0, \tag{34}$$

where,  $m_{D(\bar{D})}$  is the vacuum mass of the  $D(\bar{D})$  meson and  $\Pi_{D(\bar{D})}(\omega, |\vec{k}|)$  denotes the self-energy of the  $D(\bar{D})$  meson. For the  $D$  meson doublet ( $D^0, D^+$ ), the expression of self energy

is given as [42]

$$\begin{aligned}
\Pi_D(\omega, |\vec{k}|) &= \frac{1}{4f_D^2} \left[ 3(\rho_p + \rho_n) \pm (\rho_p - \rho_n) + 2 \left( (\rho_{\Sigma^+} + \rho_{\Sigma^-}) \pm (\rho_{\Sigma^+} - \rho_{\Sigma^-}) \right) + 2(\rho_{\Lambda^0} + \rho_{\Sigma^0}) \right. \\
&+ \left. ((\rho_{\Xi^0} + \rho_{\Xi^-}) \pm (\rho_{\Xi^0} - \rho_{\Xi^-})) \right] \omega + \frac{m_D^2}{2f_D} (\sigma' + \sqrt{2}\zeta_c' \pm \delta') \\
&+ \left[ -\frac{1}{f_D} (\sigma' + \sqrt{2}\zeta_c' \pm \delta') + \frac{d_1}{2f_D^2} (\rho_s^p + \rho_s^n + \rho_s^{\Lambda^0} + \rho_s^{\Sigma^+} + \rho_s^{\Sigma^0} + \rho_s^{\Sigma^-} + \rho_s^{\Xi^0} + \rho_s^{\Xi^-}) \right. \\
&+ \left. \frac{d_2}{4f_D^2} \left( (\rho_s^p + \rho_s^n) \pm (\rho_s^p - \rho_s^n) + \frac{1}{3}\rho_s^{\Lambda^0} + (\rho_s^{\Sigma^+} + \rho_s^{\Sigma^-}) \pm (\rho_s^{\Sigma^+} - \rho_s^{\Sigma^-}) + \rho_s^{\Sigma^0} \right) \right] (\omega^2 - \vec{k}^2).
\end{aligned} \tag{35}$$

The  $\pm$  signs in the above equation refer to the  $D^0$  and  $D^+$  mesons, respectively. Also,  $\sigma' (= \sigma - \sigma_0)$ ,  $\zeta_c' (= \zeta_c - \zeta_{c0})$ , and  $\delta' (= \delta - \delta_0)$  are the fluctuations of the scalar-isoscalar fields  $\sigma$ ,  $\zeta_c$  and the scalar-isovector field  $\delta$  from their vacuum expectation values in the strange hyperonic medium. The vacuum expectation value of  $\delta$  is zero ( $\delta_0 = 0$ ), since a nonzero value for it will break the isospin-symmetry of the vacuum. Since  $\zeta_c$  is made of heavy charm quark-antiquark pair, its medium modification is not considered in the present work, i.e,  $\zeta_c' = 0$  is assumed [39, 42]. For the  $\bar{D}$  meson doublet ( $\bar{D}^0, D^-$ ), the self-energy is given as

$$\begin{aligned}
\Pi_{\bar{D}}(\omega, |\vec{k}|) &= -\frac{1}{4f_D^2} \left[ 3(\rho_p + \rho_n) \pm (\rho_p - \rho_n) + 2 \left( (\rho_{\Sigma^+} + \rho_{\Sigma^-}) \pm (\rho_{\Sigma^+} - \rho_{\Sigma^-}) \right) + 2(\rho_{\Lambda^0} + \rho_{\Sigma^0}) \right. \\
&+ \left. ((\rho_{\Xi^0} + \rho_{\Xi^-}) \pm (\rho_{\Xi^0} - \rho_{\Xi^-})) \right] \omega + \frac{m_{\bar{D}}^2}{2f_D} (\sigma' + \sqrt{2}\zeta_c' \pm \delta') \\
&+ \left[ -\frac{1}{f_D} (\sigma' + \sqrt{2}\zeta_c' \pm \delta') + \frac{d_1}{2f_D^2} (\rho_s^p + \rho_s^n + \rho_s^{\Lambda^0} + \rho_s^{\Sigma^+} + \rho_s^{\Sigma^0} + \rho_s^{\Sigma^-} + \rho_s^{\Xi^0} + \rho_s^{\Xi^-}) \right. \\
&+ \left. \frac{d_2}{4f_D^2} \left( (\rho_s^p + \rho_s^n) \pm (\rho_s^p - \rho_s^n) + \frac{1}{3}\rho_s^{\Lambda^0} + (\rho_s^{\Sigma^+} + \rho_s^{\Sigma^-}) \pm (\rho_s^{\Sigma^+} - \rho_s^{\Sigma^-}) + \rho_s^{\Sigma^0} \right) \right] (\omega^2 - \vec{k}^2).
\end{aligned} \tag{36}$$

where the  $\pm$  sign refers to the  $\bar{D}^0(D^-)$  meson.

The in-medium mass  $m_{D(\bar{D})}^*$  for  $D(\bar{D})$  meson is obtained by solving the dispersion relation given by equation (34) for momentum  $|\vec{k}| = 0$ . The medium modifications of the masses of these open charm mesons arise due to their interactions with the scalar mesons and baryons (through their number and scalar densities). It may be noted here that there is no contribution due to interaction with the pions, since the expectation values of these odd-parity fields are zero in the mean field approximation. For the charged  $D$  ( $D^\pm$ ) mesons,

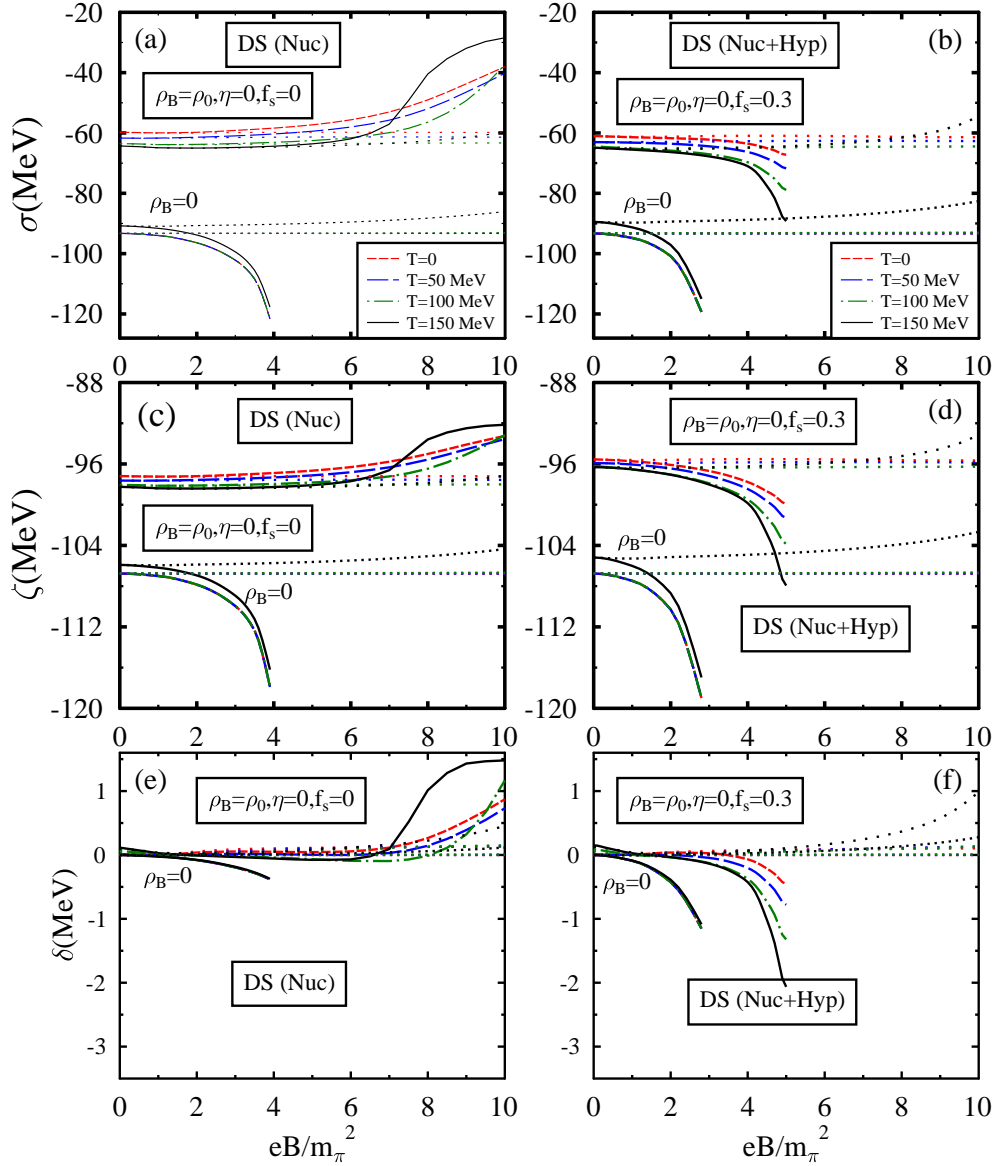


FIG. 1: The scalar fields  $\sigma$ ,  $\zeta$  and  $\delta$  are plotted as functions of magnetic field  $eB/m_\pi^2$  for  $\rho_B = 0$  and  $\rho_B = \rho_0$  (for symmetric ( $\eta = 0$ ) nuclear matter ( $f_s = 0$ ) (in subplots (a), (c) and (e)) and for hyperonic matter (with  $f_s = 0.3$ ) (in subplots (b), (d) and (f))) for different temperatures, considering baryonic Dirac sea (DS) contributions. These are also plotted when the DS contributions are ignored (the closely and widely spaced dotted lines for  $\rho_B = 0$  and  $\rho_B = \rho_0$ ).

additional contributions from the lowest Landau levels (LLL) are taken into account, and the effective mass of these mesons are given as  $m_{D_\pm}^{eff} = \sqrt{m_{D_\pm}^{*2} + |eB|}$  [56].

The effective mass of charmonium state  $\psi(3770)$  is obtained from the medium modification of the dilaton field,  $\chi$ , which simulates the gluon condensates of QCD within the



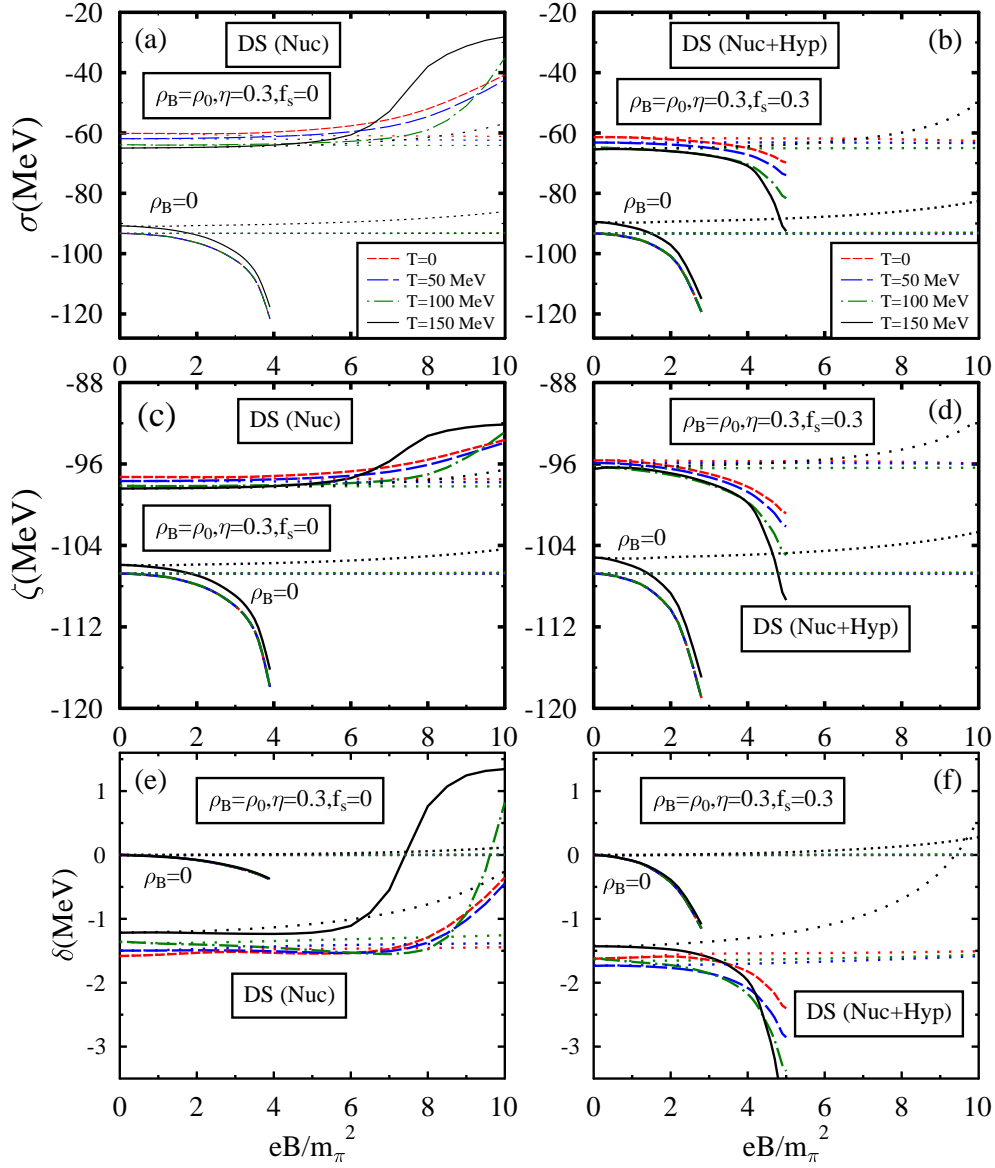


FIG. 2: Same as figure 1, for asymmetric matter ( $\eta=0.3$ ).

chiral effective model. The mass shift of the charmonium states arises from the medium modification of the scalar gluon condensate in the leading order and is given as [82–85]

$$\Delta m_\Psi = \frac{1}{18} \int d|\mathbf{k}|^2 \left\langle \left| \frac{\partial \psi(\mathbf{k})}{\partial \mathbf{k}} \right|^2 \right\rangle \frac{|\mathbf{k}|}{|\mathbf{k}|^2/m_c + \epsilon} \left( \left\langle \frac{\alpha_s}{\pi} G_{\mu\nu}^a G^{\mu\nu a} \right\rangle - \left\langle \frac{\alpha_s}{\pi} G_{\mu\nu}^a G^{\mu\nu a} \right\rangle_0 \right), \quad (37)$$

where

$$\left\langle \left| \frac{\partial \psi(\mathbf{k})}{\partial \mathbf{k}} \right|^2 \right\rangle = \frac{1}{4\pi} \int \left| \frac{\partial \psi(\mathbf{k})}{\partial \mathbf{k}} \right|^2 d\Omega. \quad (38)$$

Equating the trace of the energy momentum tensor of the chiral model and QCD relates the

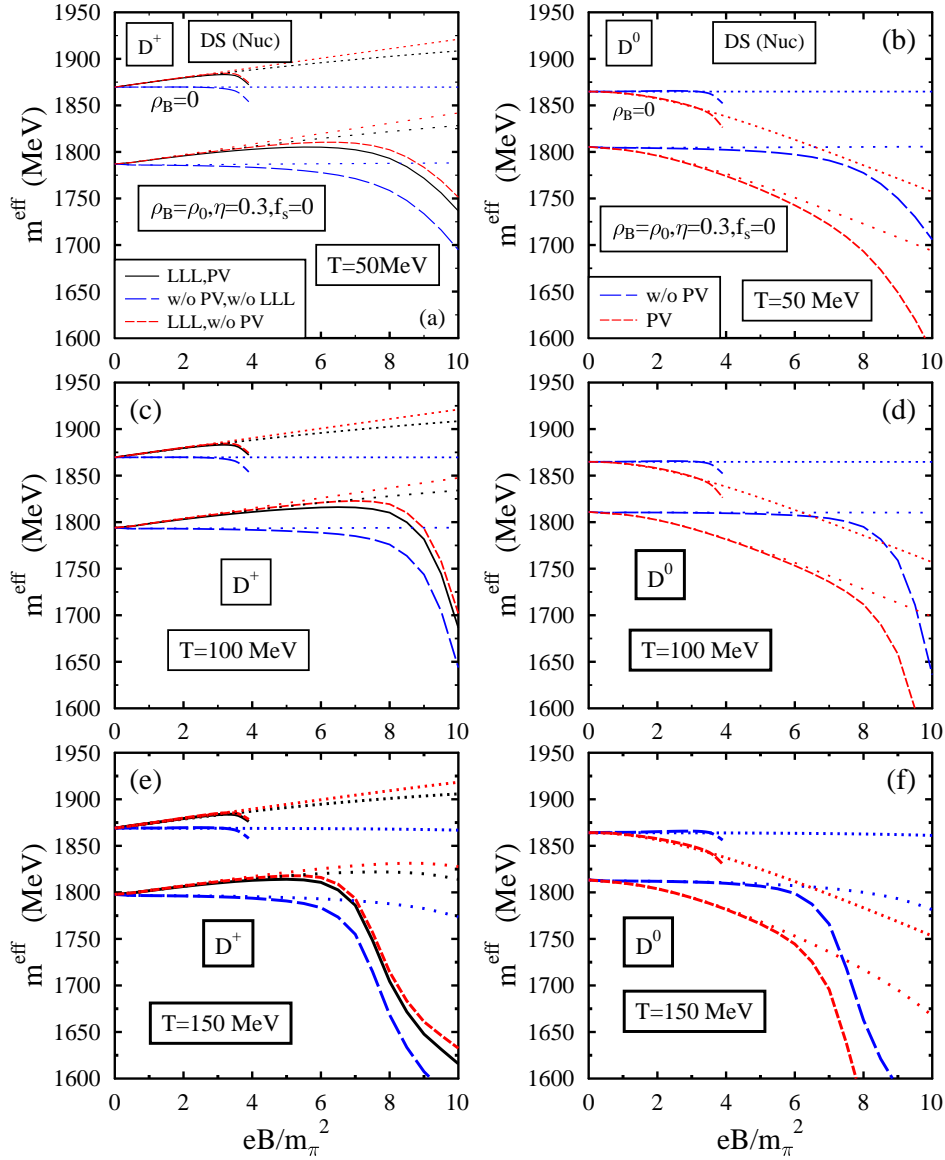


FIG. 3: The masses of pseudoscalar  $D^+$  (in subplots (a), (c) and (e)) and  $D^0$  (in subplots (b), (d) and (f)) mesons are plotted as functions of magnetic field  $eB/m_\pi^2$ , at  $T=50, 100$  and  $150$  MeV respectively, for  $\rho_B = 0$  and for asymmetric nuclear matter ( $\rho_B = \rho_0$ ,  $\eta = 0.3$  and  $f_s = 0$ ), considering baryonic Dirac sea contributions, with and without PV mixing. These are also plotted when Dirac sea contributions are neglected (the closely and widely spaced dotted lines for  $\rho_B = 0$  and  $\rho_B = \rho_0$ ).

scalar gluon condensates to the dilaton field,  $\chi$  as [42]

$$\left\langle \frac{\alpha_s}{\pi} G_{\mu\nu}^a G^{\mu\nu a} \right\rangle = \frac{24}{(33 - 2N_f)} (1 - d) \chi^4, \quad (39)$$

in the limiting situation of massless quarks in the energy momentum tensor of QCD.

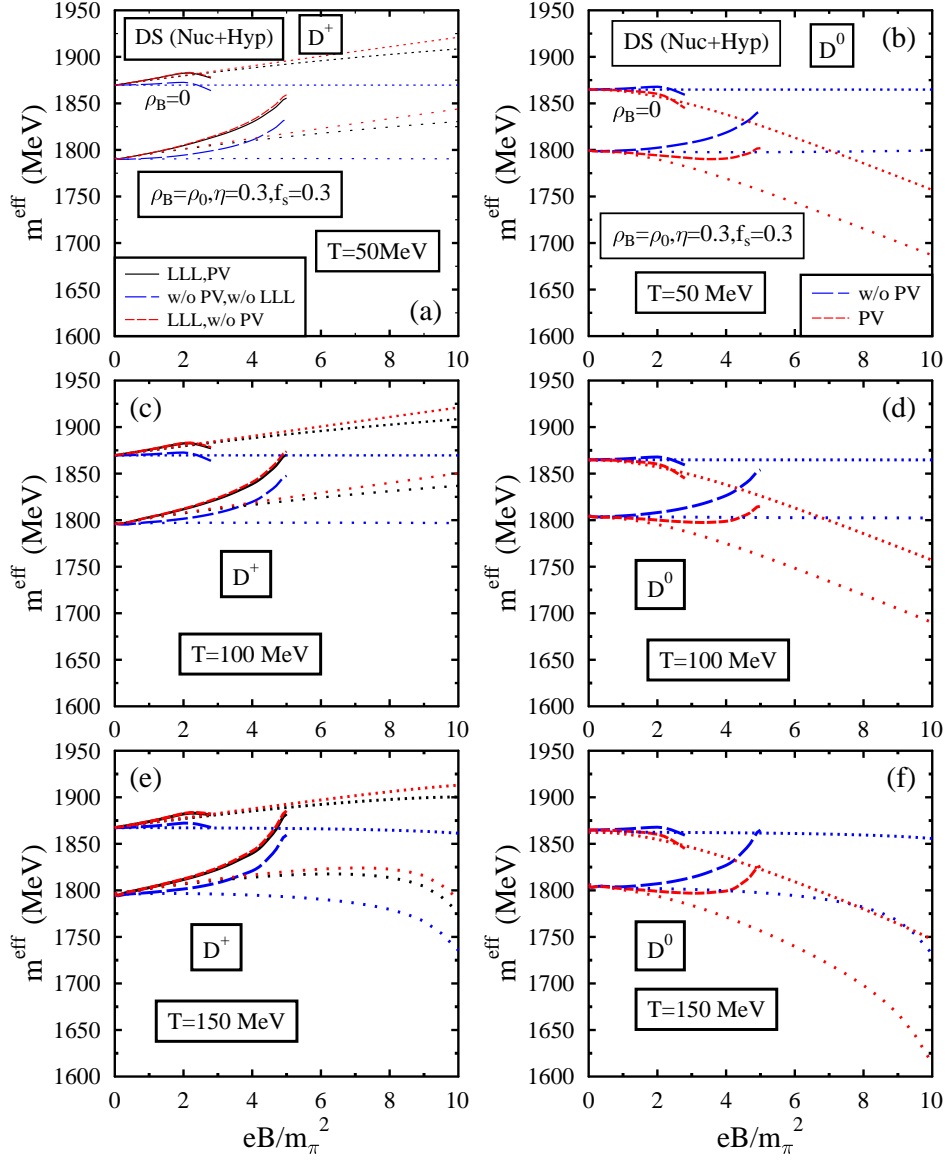


FIG. 4: Same as figure 3, for hyperonic matter (with  $f_s=0.3$ ).

Using equations (37) and (39), one obtains the mass shift of the charmonium state as [40, 42]

$$\Delta m_\Psi = \frac{4}{81}(1-d) \int d|\mathbf{k}|^2 \left\langle \left| \frac{\partial \psi(\mathbf{k})}{\partial \mathbf{k}} \right|^2 \right\rangle \frac{|\mathbf{k}|}{|\mathbf{k}|^2/m_c + \epsilon} (\chi^4 - \chi_0^4). \quad (40)$$

In equation (40),  $d$  is a parameter introduced in the scale breaking term in the Lagrangian,  $\chi$  and  $\chi_0$  are the values of the dilaton field in the magnetized medium and in vacuum respectively. The wave functions of the charmonium states,  $\psi(\mathbf{k})$  are assumed to be harmonic oscillator wave functions,  $m_c$  is the mass of the charm quark,  $\epsilon = 2m_c - m_\psi$  is the binding energy of the charmonium state of mass,  $m_\psi$ .

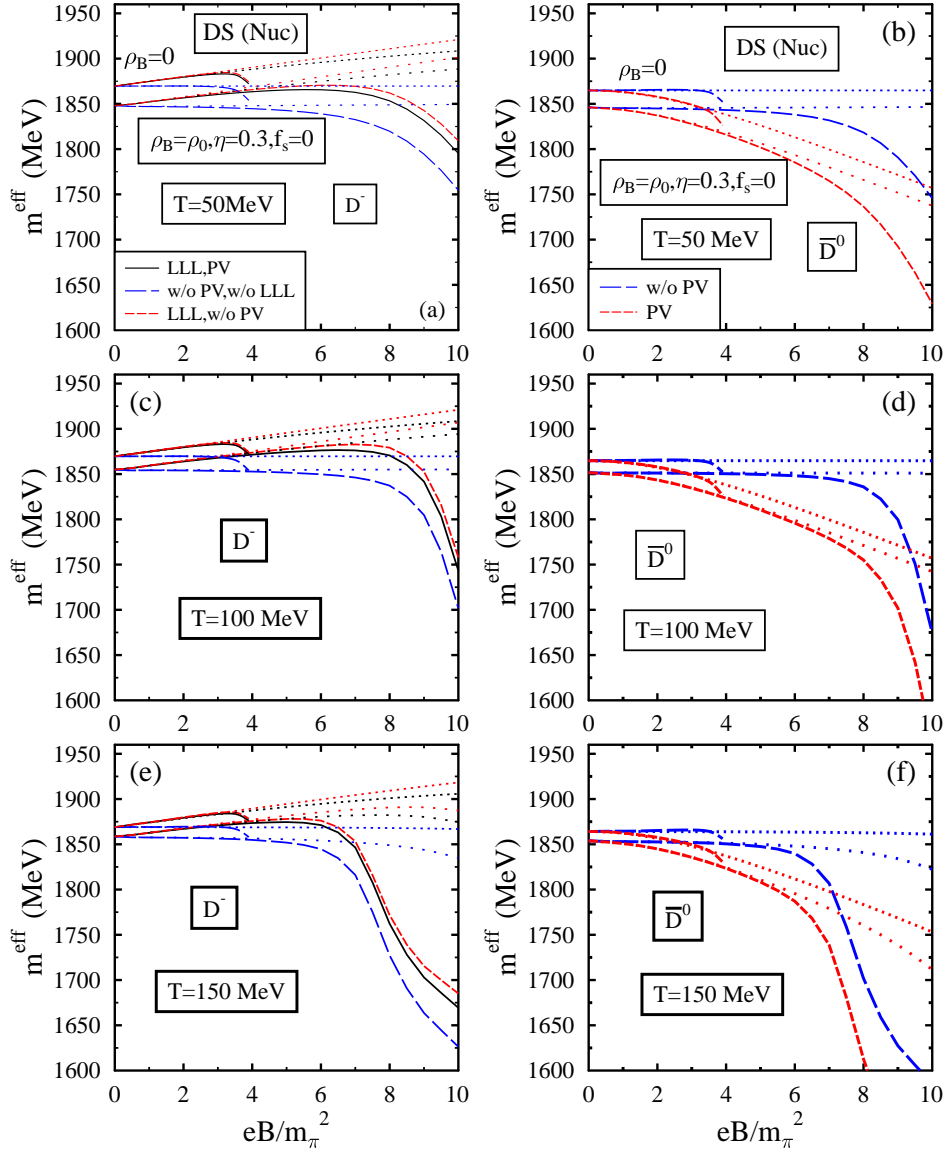


FIG. 5: The masses of pseudoscalar  $D^-$  (in subplots (a), (c) and (e)) and  $\bar{D}^0$  (in subplots (b), (d) and (f)) mesons are plotted as functions of magnetic field  $eB/m_\pi^2$ , at  $T=50, 100$  and  $150$  MeV respectively, for  $\rho_B = 0$  and for asymmetric nuclear matter ( $\rho_B = \rho_0$ ,  $\eta = 0.3$  and  $f_s = 0$ ), considering baryonic Dirac sea contributions, with and without PV mixing. These are also plotted when Dirac sea contributions are neglected (the closely and widely spaced dotted lines for  $\rho_B = 0$  and  $\rho_B = \rho_0$ ).

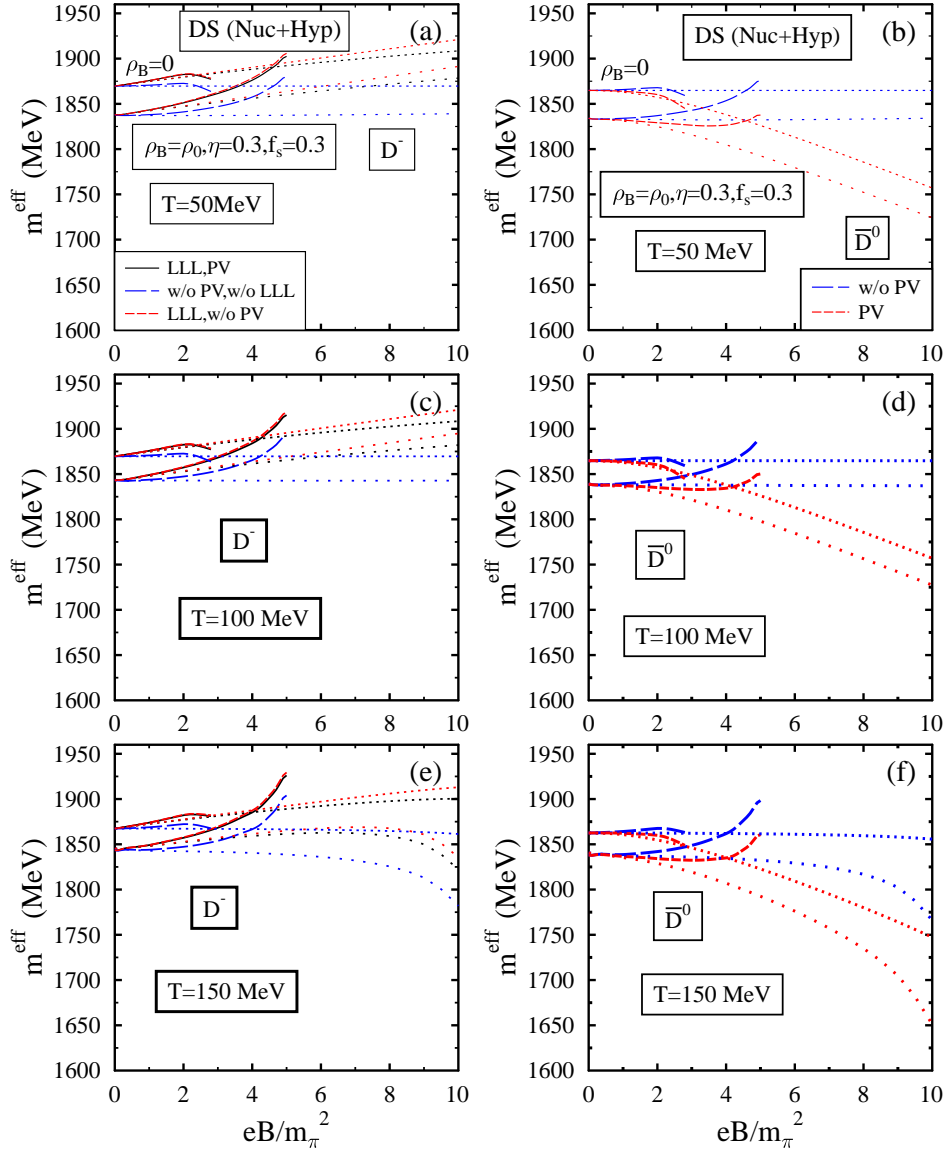


FIG. 6: Same as figure 5, for hyperonic matter (with  $f_s=0.3$ ).

### Pseudoscalar-Vector meson (PV) mixing:

In the presence of a magnetic field, there is mixing between the spin 0 (pseudoscalar) meson and spin 1 (vector) mesons, which modifies the masses of these mesons [56, 57, 86–91]. The mass modifications have been studied using a phenomenological Lagrangian density of the form [87, 88, 91]

$$\mathcal{L}_{PV\gamma} = \frac{g_{PV}}{m_{av}} e\tilde{F}_{\mu\nu}(\partial^\mu P)V^\nu, \quad (41)$$

for the heavy quarkonia [57, 58, 86–88], the open charm mesons [56] and the strange ( $K$  and  $\bar{K}$ ) mesons [90]. In equation (41),  $m_{av} = (m_V + m_P)/2$ ,  $m_P$  and  $m_V$  are the masses for

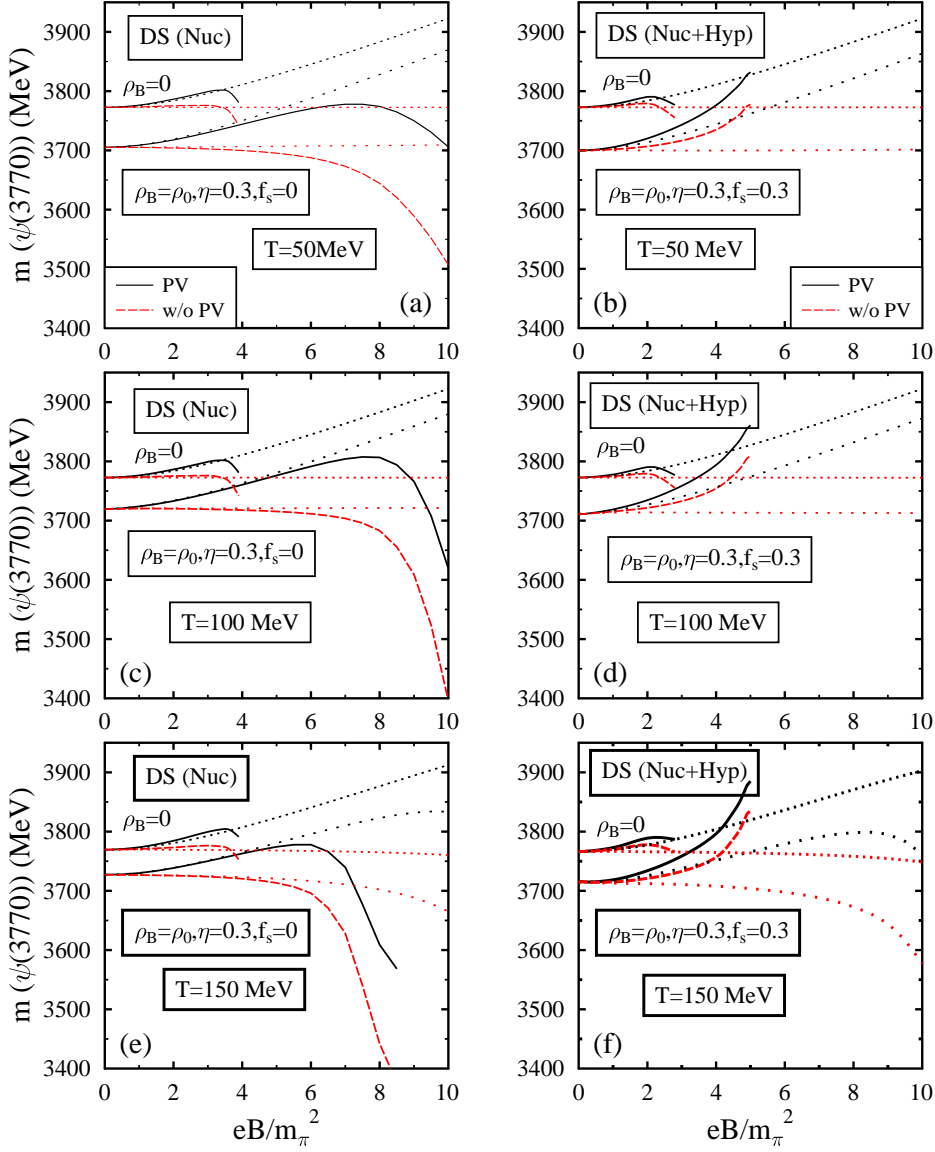


FIG. 7: The mass of charmonium  $\psi(3770)$  is plotted as a function of magnetic field  $eB/m_\pi^2$  for  $\rho_B = 0$  and for asymmetric ( $\eta = 0.3$ ) nuclear matter ( $f_s=0$ ) (in subplots (a), (c) and (e)) and strange hadronic matter (with  $f_s = 0.3$ ) (in subplots (b), (d) and (f)) at  $T=50, 100$  and  $150$  MeV respectively, for  $\rho_B = \rho_0$ , with and without PV mixing, considering baryonic Dirac sea contributions. The masses are also plotted when Dirac sea contributions are neglected (the closely and widely spaced dotted lines for  $\rho_B = 0$  and  $\rho_B = \rho_0$ ).

the pseudoscalar and vector charmonium states,  $\tilde{F}_{\mu\nu}$  is the dual electromagnetic field. The coupling parameter  $g_{PV}$  is fitted from the observed value of the radiative decay width,  $\Gamma(V \rightarrow P + \gamma)$ . Assuming the spatial momenta of the heavy quarkonia to be zero, there is observed

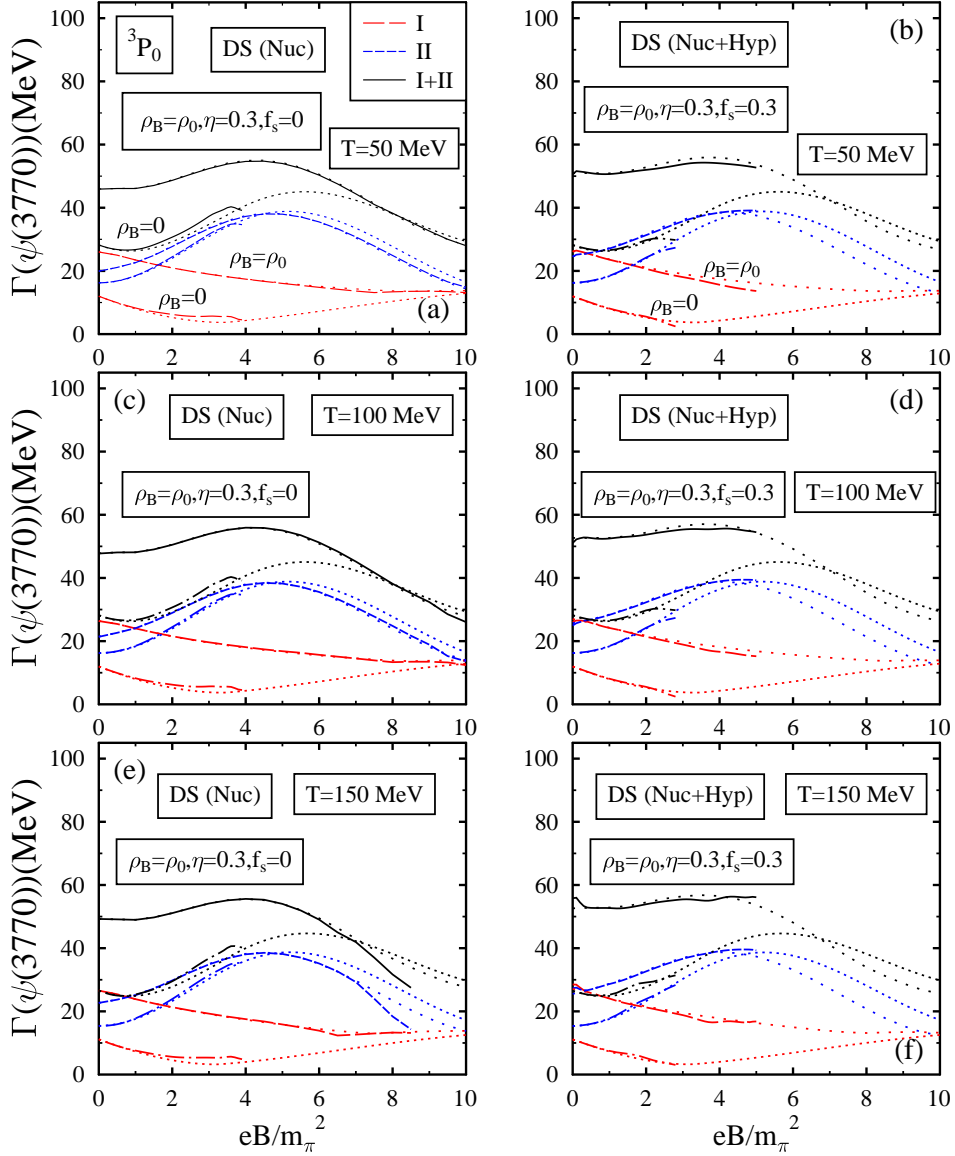


FIG. 8: Decay widths of charmonium  $\psi(3770)$  to (I)  $D^+D^-$ , (II)  $D^0\bar{D}^0$  and (III) total  $D\bar{D}$ , i.e., (I+II) are plotted as functions of magnetic field  $eB/m_\pi^2$  for  $\rho_B = 0$  and for asymmetric ( $\eta = 0.3$ ) nuclear matter ( $f_s = 0$ ) (in subplots (a), (c) and (e)) and strange hadronic matter ( $f_s=0.3$ ) (in subplots (b), (d) and (f)) at  $T=50, 100$  and  $150$  MeV respectively, for  $\rho_B = \rho_0$ , using the  $^3P_0$  model, considering baryonic Dirac sea contributions and PV mixing. These are also plotted when Dirac sea contributions are neglected (the closely and widely spaced dotted lines for  $\rho_B = 0$  and  $\rho_B = \rho_0$ ).

to be mixing between the pseudoscalar and the longitudinal component of the vector field from their equations of motion obtained with the phenomenological  $PV\gamma$  interaction given

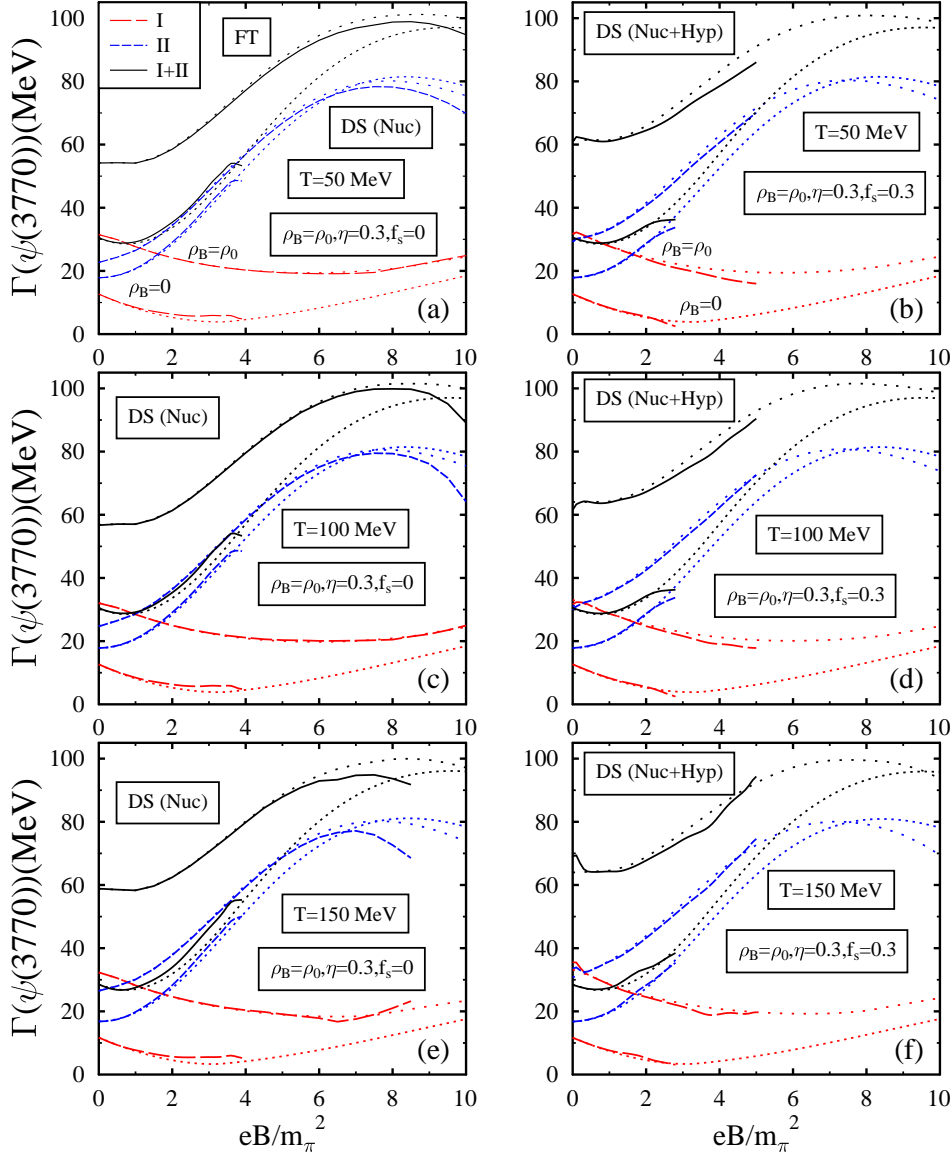


FIG. 9: Same as Fig. 8, using the field theoretical (FT) model of composite hadrons.

by equation (41). The physical masses of the pseudoscalar and the longitudinal component of the vector mesons including the mixing effects, obtained by solving their equations of motion, are given as [87, 88, 91]

$$m_{P(V||)}^{(PV)} = \frac{1}{2} \left( M_+^2 + \frac{c_{PV}^2}{m_{av}^2} \mp \sqrt{M_-^4 + \frac{2c_{PV}^2 M_+^2}{m_{av}^2} + \frac{c_{PV}^4}{m_{av}^4}} \right), \quad (42)$$

where  $M_+^2 = m_P^2 + m_V^2$ ,  $M_-^2 = m_V^2 - m_P^2$  and  $c_{PV} = g_{PV}eB$ . In the above equation, the ‘ $\mp$ ’ corresponds to the mass of the pseudoscalar (longitudinal component of the vector) meson. The effective Lagrangian term given by equation (41) has been observed to lead to



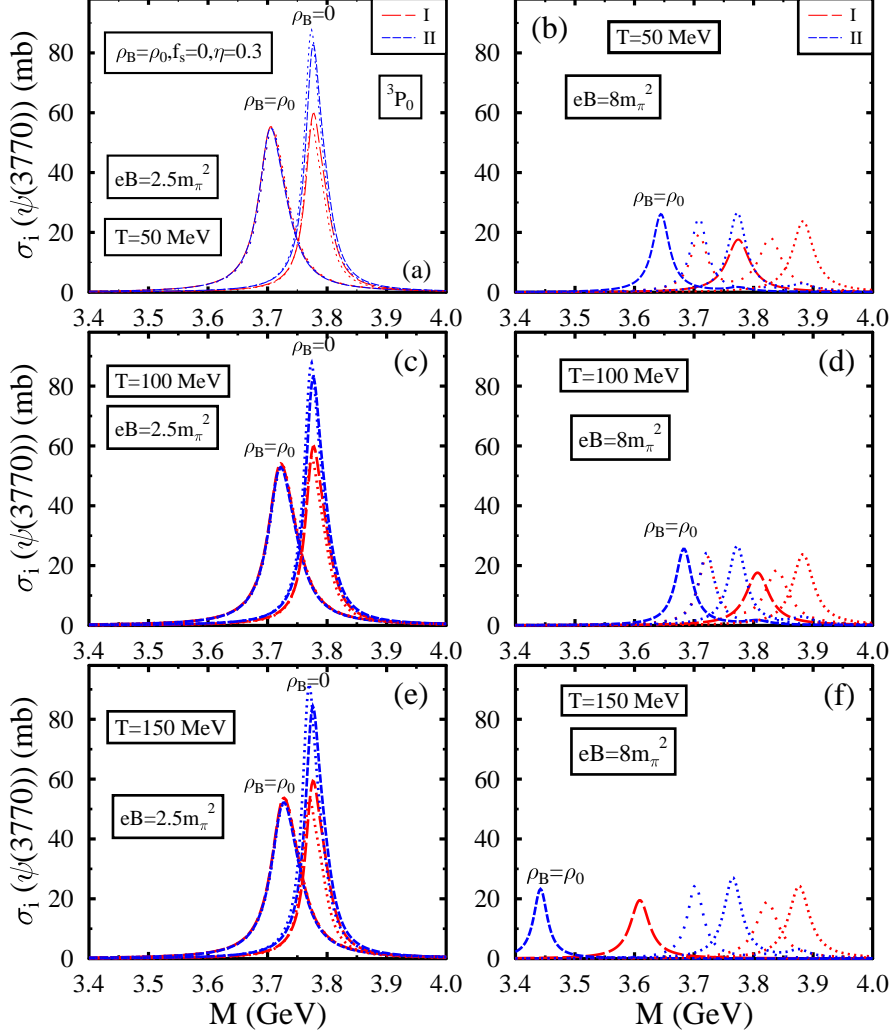


FIG. 10: Production cross-sections of  $\psi(3770)$  due to scattering of (I)  $D^+D^-$  and (II)  $D^0\bar{D}^0$  mesons are plotted as functions of the invariant mass, for  $eB = 2.5m_\pi^2$  (in subplots (a), (c) and (e)) and  $eB = 8m_\pi^2$  (in subplots (b), (d) and (f)) at  $T=50, 100$  and  $150$  MeV respectively, for  $\rho_B = 0$  as well as for asymmetric ( $\eta=0.3$ ) nuclear ( $f_s=0$ ) matter at  $\rho_B = \rho_0$ , with the decay widths obtained using the  $^3P_0$  model. These are also plotted when Dirac sea contributions are neglected (the closely and widely spaced dotted lines for  $\rho_B = 0$  and  $\rho_B = \rho_0$ ).

the mass modifications of the longitudinal  $J/\psi$  and  $\eta_c$  due to the presence of the magnetic field, which agree extremely well with a study of these charmonium states using a QCD sum rule approach incorporating the mixing effects [86, 87].

The PV mixing effects for the open charm mesons (due to  $D - D^*$  and  $\bar{D} - \bar{D}^*$  mixings) [56], in addition to the mixing of the charmonium states (due to  $J/\psi - \eta_c$ ,  $\psi' - \eta'_c$  and  $\psi(3770) - \eta'_c$  mixings) [56, 57], as calculated using the phenomenological Lagrangian given

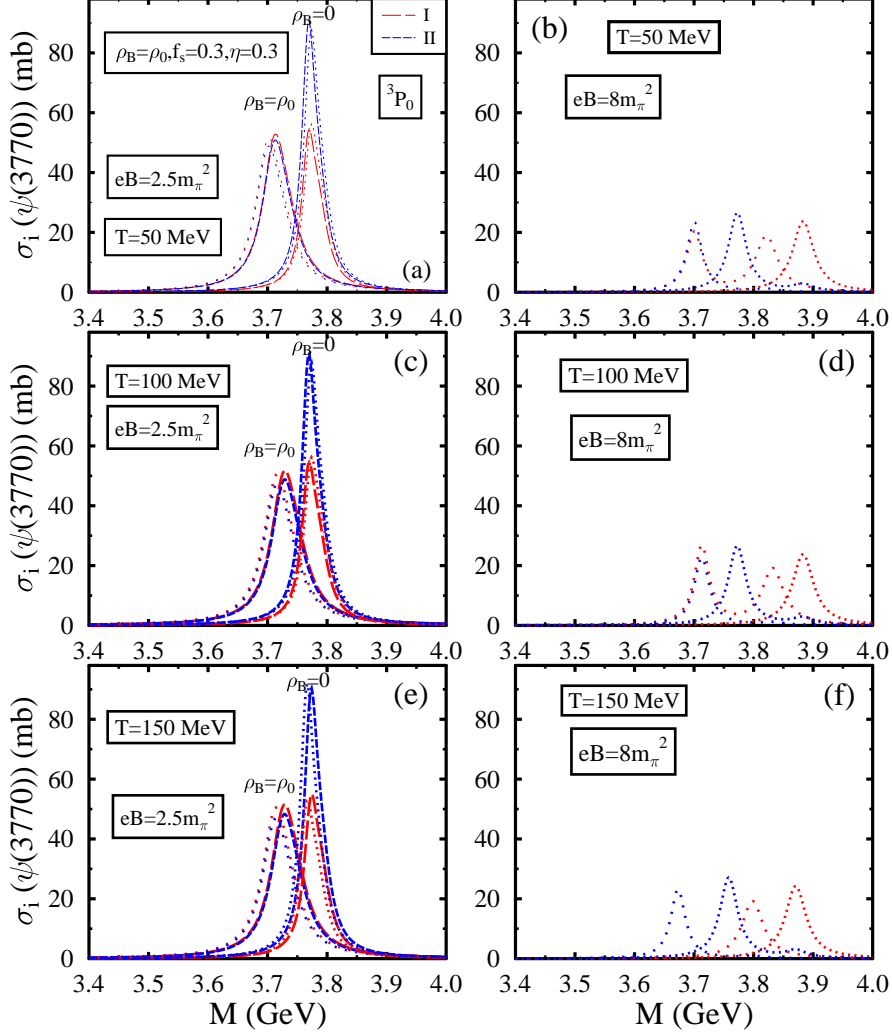


FIG. 11: Same as Fig. 10, for strange hadronic matter (with  $f_s=0.3$ ).

by equation (41) have been observed to lead to appreciable drop (rise) in the mass of the pseudoscalar (longitudinal component of the vector) meson. These were observed to modify the partial decay width of  $\psi(3770) \rightarrow D\bar{D}$  [56, 57], with the modifications being much more dominant due to the PV mixing in the open charm ( $D - D^*$  and  $\bar{D} - \bar{D}^*$ ) mesons.

### B. Partial Decay width of Charmonium state to $D\bar{D}$

In this subsection, we briefly describe the study of partial decay width of charmonium state,  $\psi(3770)$  to open charm ( $D$  and  $\bar{D}$ ) mesons, in hot asymmetric strange hadronic matter in the presence of a magnetic field. These are studied using (I) the  ${}^3P_0$  model, and, (II) a field theoretical (FT) model of composite hadrons with quark (and antiquark) constituents. In both of these models, the decay proceeds with creation of a light quark-antiquark pair

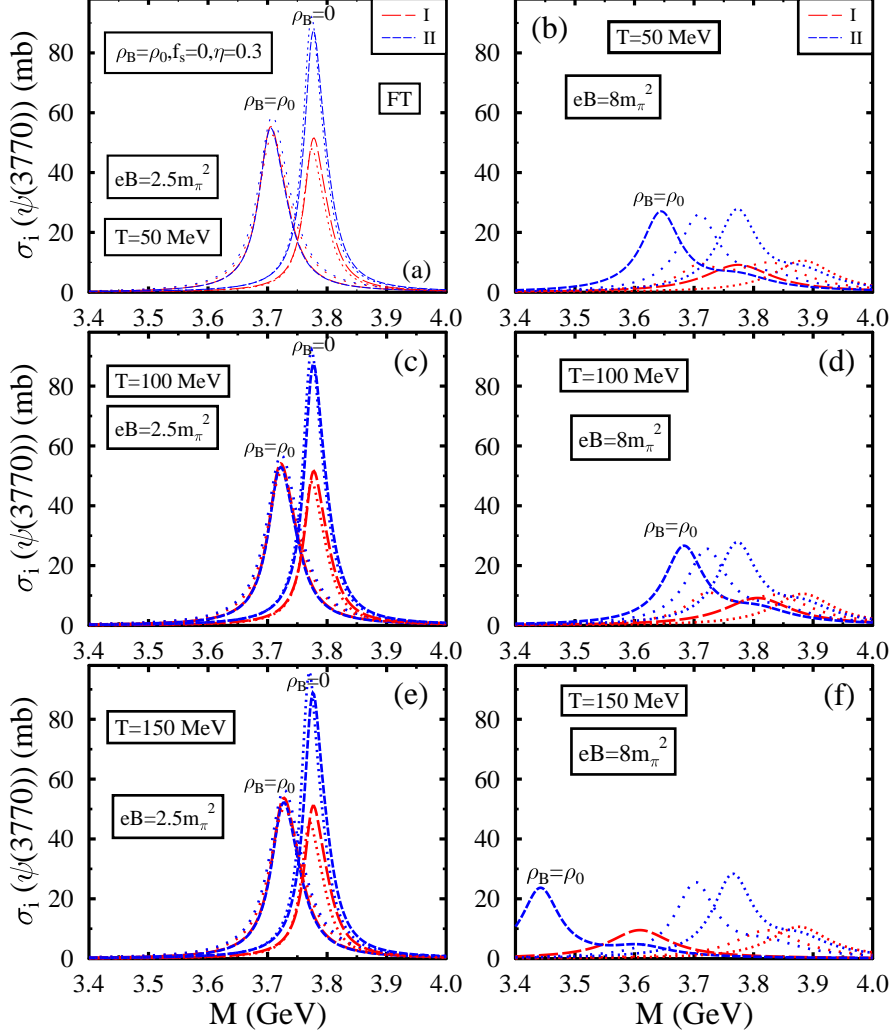


FIG. 12: Same as Fig. 10, with decay widths calculated using the field theoretical (FT) model of composite hadrons.

and the heavy charm quark (antiquark) of the parent charmonium state combining with the light antiquark (quark) to produce the  $D\bar{D}$  in the final state.

For the charmonium state decaying at rest, the in-medium decay widths are obtained in terms of the magnitude of the 3-momentum of the outgoing  $D$  ( $\bar{D}$ ) given as

$$|\mathbf{p}| = \left( \frac{M_\psi^2}{4} - \frac{m_D^2 + m_{\bar{D}}^2}{2} + \frac{(m_D^2 - m_{\bar{D}}^2)^2}{4M_\psi^2} \right)^{1/2}, \quad (43)$$

where,  $M_\psi$ ,  $m_D$  and  $m_{\bar{D}}$  are the in-medium masses of the charmonium state,  $\psi(3770)$ ,  $D$  and  $\bar{D}$  mesons. The mass modifications of the charmonium states and the open charm mesons are observed to lead to substantial modification of the partial decay width of  $\psi(3770) \rightarrow D\bar{D}$  [57] due to  $\psi(3770) - \eta'_c$  mixing, as well as, due to  $D(\bar{D}) - D^*(\bar{D}^*)$  mixing effects [56, 62]. The

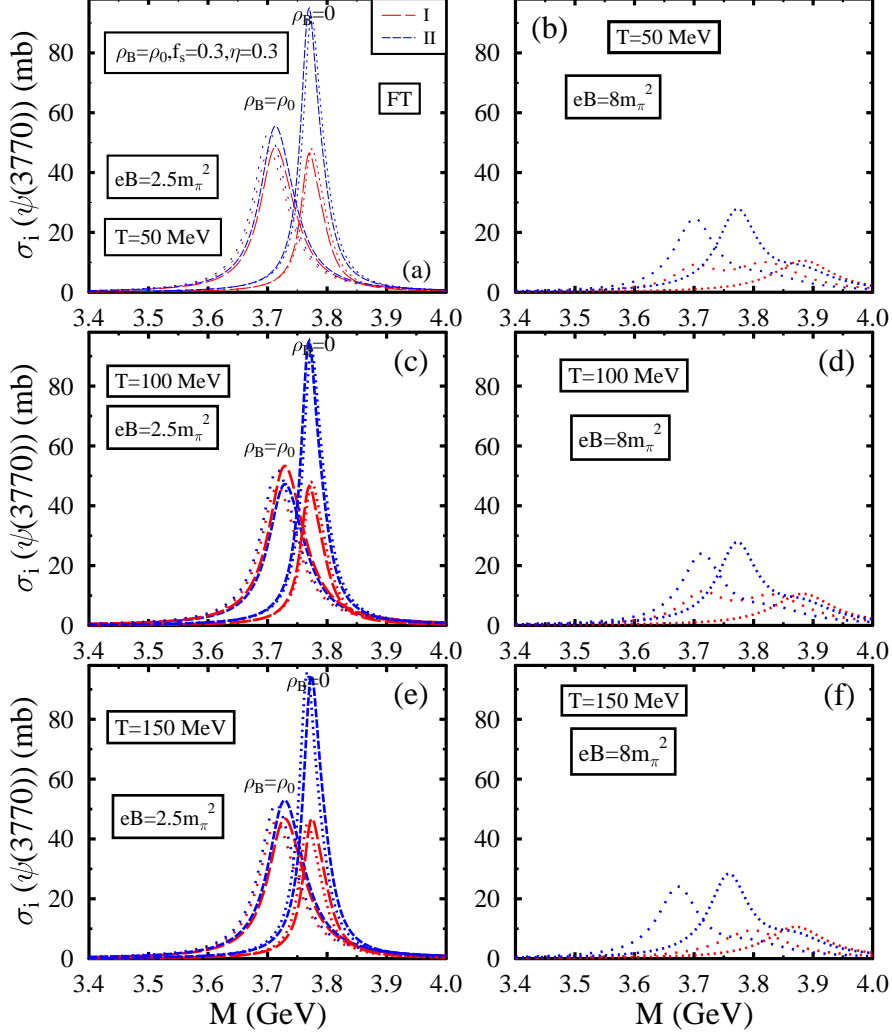


FIG. 13: Same as Fig. 11, with decay widths calculated using the field theoretical (FT) model of composite hadrons.

medium modified masses of  $D$ ,  $\bar{D}$  mesons and the charmonium state  $\psi(3770)$  in magnetized isospin asymmetric strange hadronic matter at finite temperatures, and, their effect on the decay width of  $\psi(3770) \rightarrow D\bar{D}$  are calculated in the present investigation. The masses of the charmonium and open charm mesons are computed including the effects of the Dirac sea as well as PV mixing, with additional contributions from the lowest Landau level (LLL) for the charged  $D^\pm$  mesons, as has been described in the previous subsections.

The  $^3P_0$  model [66, 92–94] describes the charmonium decaying to  $D\bar{D}$  with creation of a light quark-antiquark pair in the  $^3P_0$  state, where the light quark and antiquark combine with the heavy charm antiquark and quark of the parent meson, to produce the  $D$  and  $\bar{D}$  mesons in the final state. The wave functions of the charmonium state and the open charm

mesons are assumed to be of harmonic oscillator type. The decay width of the charmonium state  $\psi(3770)$ , corresponding to the  $1D$  state, decaying at rest to  $D\bar{D}$  is given as [66, 94]

$$\Gamma^{[{}^3P_0]}(\psi(3770)(\mathbf{0}) \rightarrow D(\mathbf{p})\bar{D}(-\mathbf{p})) = \pi^{1/2} \frac{E_D(|\mathbf{p}|)E_{\bar{D}}(|\mathbf{p}|)\gamma^2 2^{11}5}{2M_\psi 3^2} \left(\frac{r}{1+2r^2}\right)^7 \times x^3 \left(1 - \frac{1+r^2}{5(1+2r^2)}x^2\right)^2 \exp\left(-\frac{x^2}{2(1+2r^2)}\right), \quad (44)$$

where,  $x = |\mathbf{p}|/\beta_D$ ,  $r = \frac{\beta}{\beta_D}$  is the ratio of the harmonic oscillator strengths of the decaying charmonium state and the produced  $D(\bar{D})$ -mesons,  $E_D(|\mathbf{p}|)$  and  $E_{\bar{D}}(|\mathbf{p}|)$  is the energy of the outgoing  $D(\bar{D})$  meson given as  $E_{D(\bar{D})}(|\mathbf{p}|) = (|\mathbf{p}|^2 + m_{D(\bar{D})}^2)^{1/2}$ , and,  $\gamma$  is a measure of the strength of the  ${}^3P_0$  vertex [66, 94] fitted from the observed decay width of  $\psi(3770) \rightarrow D\bar{D}$  [42].

We next briefly describe the field theoretical model of composite hadrons [67, 68] used to compute the partial decay widths of  $\psi(3770) \rightarrow D\bar{D}$  in magnetized hot isospin asymmetric hyperonic matter. The model describes the hadrons as comprising of quark (and antiquark) constituents. The constituent quark field operators of the hadron in motion are constructed from the constituent quark field operators of the hadron at rest, by a Lorentz boosting. Similar to the MIT bag model [95], where the quarks (antiquarks) occupy specific energy levels inside the hadron, it is assumed in the present model for the composite hadrons that the quark (antiquark) constituents carry fractions of the mass (energy) of the hadron at rest (in motion) [67, 68]. With explicit constructions of the charmonium state and the open charm ( $D$  and  $\bar{D}$ ) mesons, the charmonium decay width is calculated using the light quark antiquark pair creation term of the free Dirac Hamiltonian given as

$$\mathcal{H}_{q\bar{q}}(\mathbf{x}, t=0) = Q_q^{(p)}(\mathbf{x})^\dagger (-i\vec{\alpha} \cdot \vec{\nabla} + \beta M_q) \tilde{Q}_q^{(p')}(\mathbf{x}) \quad (45)$$

where,  $\vec{\alpha} = \begin{pmatrix} 0 & \vec{\sigma} \\ \vec{\sigma} & 0 \end{pmatrix}$  and  $\beta = \begin{pmatrix} I & 0 \\ 0 & -I \end{pmatrix}$  are the Dirac matrices,  $M_q$  is the constituent mass of the light quark (antiquark). The subscript  $q$  of the field operators in equation (45) refers to the fact that the light antiquark,  $\bar{q}$  and light quark,  $q$  are the constituents of the  $D$  and  $\bar{D}$  mesons with momenta  $\mathbf{p}$  and  $\mathbf{p}'$  respectively in the final state of the decay of the charmonium state,  $\Psi(3770)$ . The decay width of  $\psi(3770) \rightarrow D\bar{D}$  is calculated from the matrix element of the light quark-antiquark pair creation part of the free Dirac Hamiltonian,

between the initial and the final state mesons as given by

$$\langle D(\mathbf{p}) | \langle \bar{D}(\mathbf{p}') | \int \mathcal{H}_{q\bar{q}}(\mathbf{x}, t=0) d\mathbf{x} | \psi(3770)^m(\vec{0}) \rangle = \delta(\mathbf{p} + \mathbf{p}') A_\psi(|\mathbf{p}|) p_m, \quad (46)$$

which yields the expression for the decay width as given by

$$\Gamma^{[FT]}(\psi(3770) \rightarrow D(\mathbf{p})\bar{D}(-\mathbf{p})) = \gamma_\psi^2 \frac{8\pi^2}{3} |\mathbf{p}|^3 \frac{E_D(|\mathbf{p}|)E_{\bar{D}}(|\mathbf{p}|)}{M_\psi} A_\psi(|\mathbf{p}|)^2 \quad (47)$$

where,  $E_{D(\bar{D})}(|\mathbf{p}|) = (m_{D(\bar{D})}^2 + |\mathbf{p}|^2)^{1/2}$ , with  $|\mathbf{p}|$ , the magnitude of the momentum of the outgoing  $D(\bar{D})$  meson given by equation (43), and,  $A_\psi(|\mathbf{p}|)$  is a polynomial in  $|\mathbf{p}|$ . The parameter  $\gamma_\psi$  is adjusted to reproduce the vacuum decay widths of  $\psi(3770)$  to  $D^+D^-$  and  $D^0\bar{D}^0$  [69].

We might note that the expressions of the decay widths calculated using (I) the  $^3P_0$  model as well as (II) a field theoretical model of composite hadrons, as given by equations (44) and (47) have the forms of a polynomial multiplied by a gaussian function of  $|\mathbf{p}|$ , which depends only on the masses of the charmonium and the  $D(\bar{D})$  mesons, as can be seen from equation (43). Within the  $^3P_0$  model, the polynomial dependence was observed to lead to an initial increase followed by a drop and even vanishing of the decay width with increase in the baryon density, in spite of the drop in the masses of the outgoing  $D$  and  $\bar{D}$  mesons [42, 66]. A similar behaviour of an initial increase of the decay width of  $\psi(3770)$  to the neutral  $D\bar{D}$  pair with increase in the magnetic field followed by a drop is observed in the magnetized hot nuclear (hyperonic) matter in the present work for both the models. As has already been mentioned, the masses of the  $D$ ,  $\bar{D}$  and the charmonium state,  $\psi(3770)$  are the in-medium masses in the magnetized hot asymmetric nuclear (hyperonic) matter calculated in the chiral effective model. These are computed including the effects of the Dirac sea of baryons and due to PV mixing with additional contributions from lowest Landau levels for the charged open charm mesons [62].

Including the PV mixing effect, the expression for the decay width is modified to

$$\begin{aligned} \Gamma_{PV}^{[{}^3P_0][FT]}(\psi(3770)(\mathbf{0}) \rightarrow D(\mathbf{p})\bar{D}(-\mathbf{p})) &= \frac{2}{3} \Gamma^{[{}^3P_0][FT]}(\psi(3770) \rightarrow D(\mathbf{p})\bar{D}(-\mathbf{p})) \\ &+ \frac{1}{3} \Gamma^{[{}^3P_0][FT]}(\psi(3770) \rightarrow D(\mathbf{p})\bar{D}(-\mathbf{p})) (|\mathbf{p}| \rightarrow |\mathbf{p}|(M_\psi = M_\psi^{PV})), \end{aligned} \quad (48)$$

where,  $\Gamma(\psi(3770) \rightarrow D(\mathbf{p})\bar{D}(-\mathbf{p}))$  is given by expressions (44) and (47) for computation using (I) the  $^3P_0$  model and (II) the field theoretical (FT) model of composite hadrons. In

equation (48), the first term corresponds to the transverse polarizations for the charmonium state,  $\psi(3770)$  whose masses remain unaffected by the PV mixing, whereas, the second term corresponds to the longitudinal component, whose mass is modified due to the mixing with the pseudoscalar meson in the presence of the magnetic field.

### C. Production Cross-sections of Charmonium state $\psi(3770)$

The production cross-section of vector meson,  $V$ , due to scattering of particles  $a_i$  and  $b_i$  is given as [96–102]

$$\sigma_i(M) = 6\pi^2 \frac{\Gamma_V^{i*}}{q(m_V^*, m_{a_i}^*, m_{b_i}^*)^2} A_V(M), \quad (49)$$

where,

$$A_V(M) = C \cdot \frac{2}{\pi} \frac{M^2 \Gamma_V^*}{(M^2 - m_V^{*2})^2 + (M \Gamma_V^*)^2} \quad (50)$$

is the relativistic Breit Wigner spectral function expressed in terms of the invariant mass  $M$ , the mass and decay width of the vector meson,  $m_V^*$  and  $\Gamma_V^* = \sum_j \Gamma_V^{j*}$ , in the magnetized matter, and,  $m_{a_i}^*$  and  $m_{b_i}^*$  are the in-medium masses of the scattering particles  $a_i$  and  $b_i$  in channel  $i$ . In equation (49),  $q(m_V^*, m_{a_i}^*, m_{b_i}^*)$  is the momentum of the scattering particle  $a_i(b_i)$  in the center of mass frame of the vector meson,  $V$ . The normalization constant,  $C$  in the spectral function is determined from  $\int_0^\infty A_V(M) dM = 1$ . In the present work, the production cross-section of the  $\psi(3770)$  in channel  $i = I, II$  arises from the two-body scatterings of (I)  $D^+ D^-$  and (II)  $D^0 \bar{D}^0$  mesons respectively. In the magnetized hot isospin asymmetric strange hadronic matter, these are calculated accounting for the Dirac sea and PV ( $\psi(3770) - \eta'_c$ ,  $D - D^*(D^+ - D^{*+}, D^0 - D^{*0})$  and  $\bar{D} - \bar{D}^*(D^- - D^{*-}, \bar{D}^0 - \bar{D}^{*0})$ ) mixing effects for the masses of these mesons. The decay width of  $\psi(3770) \rightarrow D \bar{D}$  is obtained using the light quark antiquark pair creation models, (I)  $^3P_0$  model, as well as (II) a field theoretical model of composite hadrons, described in the previous subsection.

The PV mixing effect introduces mass difference between the longitudinal and transverse components of the vector charmonium state  $\psi(3770)$  since the longitudinal component undergoes mass modification due to mixing with the pseudoscalar meson  $\eta'_c$ , whereas the transverse component is unaffected due to PV mixing. In the presence of PV mixing, the production cross-section of the vector meson,  $V$ , is given as

$$\sigma_i(M) = 6\pi^2 \left( \frac{1}{3} \frac{\Gamma_V^{*iL}}{q(m_V^{*L}, m_{a_i}^*, m_{b_i}^*)^2} A_V^L(M) + \frac{2}{3} \frac{\Gamma_V^{*iT}}{q(m_V^{*T}, m_{a_i}^*, m_{b_i}^*)^2} A_V^T(M) \right), \quad (51)$$

for channel  $i = I, II$  corresponding to the scattering of the charged  $D^+D^-$  and neutral  $D^0\bar{D}^0$  mesons respectively. In the above equation,  $m_V^{*T(L)}$  is the mass of the transverse (longitudinal) component of the vector meson.  $\Gamma_V^{*i T(L)}$  is the decay width of the transverse (longitudinal) component of the vector meson in channel  $i$ , with the total contribution to the decay width of the transverse (longitudinal) component arising from both the channels as given by  $\Gamma_V^{*T(L)} = \Gamma_V^{*I T(L)} + \Gamma_V^{*II T(L)}$ . In equation (51),  $A_V^{T(L)}(M)$  is the contribution from the transverse (longitudinal) component to the spectral function of the vector meson, and is given as,

$$A_V^{T(L)}(M) = C \cdot \frac{2}{\pi} \frac{M^2 \Gamma_V^{*T(L)}}{\left(M^2 - m_V^{*T(L)}\right)^2 + \left(M \Gamma_V^{*T(L)}\right)^2}, \quad (52)$$

with the constant  $C$  determined from the normalization condition

$$\int_0^\infty \left( \frac{1}{3} A_V^L(M) + \frac{2}{3} A_V^T(M) \right) dM = 1. \quad (53)$$

#### IV. RESULTS AND DISCUSSIONS

In the present investigation, we study the charmonium production in magnetized hot isospin asymmetric strange hadronic matter. Strong magnetic fields are estimated to be produced in ultra-relativistic peripheral collisions where the created matter is extremely dilute. In the present study, we study the production cross-section of  $\psi(3770)$ , which is the lowest charmonium state which decays to  $D\bar{D}$  in vacuum. As has been described in the previous section, the mass modifications of the open charm ( $D$  and  $\bar{D}$ ) mesons and the charmonium state,  $\psi(3770)$  are calculated within a generalized chiral effective model [39, 40, 42]. The medium modifications of the masses of these mesons are calculated including the effects of the baryonic Dirac sea (DS). In the presence of an external magnetic field, the masses of these mesons are additionally modified due to the mixing of the pseudoscalar meson with the longitudinal component of the vector meson (PV mixing) and these modifications are observed to be quite significant for high magnetic fields. The decay width of  $\psi(3770) \rightarrow D\bar{D}$  in hot isospin asymmetric strange hadronic matter in the presence of an external magnetic field is calculated from the medium modifications of the masses of the initial and final state mesons. Using the in-medium mass and decay width, the production cross-sections of  $\psi(3770)$ , arising from scatterings of  $D^+D^-$  as well as  $D^0\bar{D}^0$  mesons, are computed from



the relativistic Breit-Wigner spectral function. As can be seen later, these production cross-sections, have distinct peak positions in the invariant mass spectra, since the longitudinal component of  $\psi(3770)$  undergoes a positive mass shift due to mixing with  $\eta_c(2S)$ , whereas, the masses of the transverse components remain unaffected by PV mixing.

The in-medium masses of the open charm mesons ( $D$  and  $\bar{D}$ ) within the chiral effective model are obtained, due to their interactions with the baryons and the scalar mesons. These are calculated by solving the dispersion relation given by equation (34), where the self energies of the  $D$  and  $\bar{D}$  are given by equations (35) and (36) respectively. Within the mean field approximation, the scalar (the nonstrange isoscalar,  $\sigma$ , the strange isoscalar  $\zeta$  and the nonstrange isovector,  $\delta$ ) fields, along with the dilaton field,  $\chi$  and the vector fields, are solved from their coupled equations of motion, given by equations (19)–(25), for given values of the temperature and the magnetic field for zero density, as well as, for hadronic matter for given baryon density, strangeness,  $f_s$  and isospin asymmetry parameter,  $\eta$ . The charmonium mass shift is obtained from the value of the dilaton field using equation (40). In the present work, the anomalous magnetic moments (AMMs) of the baryons are taken into account.

Figures 1 and 2 show the dependence of the scalar fields  $\sigma$ ,  $\zeta$  and  $\delta$  (which are related to the light quark condensates through equation (11)) on the magnetic field, for  $\rho_B = \rho_0$ , for symmetric and asymmetric (with  $\eta=0.3$ ) matter respectively. These are plotted for the cases of nuclear matter ( $f_s=0$ ) and for strange hadronic matter (with  $f_s=0.3$ ) and compared to the results with zero baryon density. In the present work, the finite anomalous magnetic moments (AMMs) of the baryons are incorporated. The values of the scalar fields are plotted with effects of the baryon Dirac sea and compared to the case when the Dirac sea effects are not considered (shown as closely and widely spaced dotted lines for  $\rho_B = 0$  and  $\rho_0$ , respectively). The effects of the strangeness in the medium is observed to lead to significant modifications to the scalar fields both for symmetric and asymmetric matter. Contrary to the case of  $\rho_B=0$  [63], for the magnetized nuclear matter ( $f_s=0$ ), at  $\rho_B = \rho_0$ , there is observed to be a decrease in the magnitude of the scalar fields  $\sigma$  ( $\sim m_u\langle\bar{u}u\rangle + m_d\langle\bar{d}d\rangle$ ) as well as  $\zeta$  ( $\sim m_s\langle\bar{s}s\rangle$ ) fields with increase in the magnetic field, an effect called the inverse magnetic catalysis, when the AMMs of the nucleons are taken into account. As has been shown in Ref. [63], the opposite effect of magnetic catalysis is observed in magnetized nuclear ( $f_s=0$ ) matter for  $\rho_B = \rho_0$  at zero temperature, when the nucleon AMMs are ignored. In

the magnetized nuclear matter, for  $\rho_B = \rho_0$ , including the contributions of the Dirac sea and anomalous magnetic moments of the nucleons leads to the inverse magnetic catalysis effect, also at finite temperatures. For magnetic field  $eB = 4m_\pi^2$ , the values of scalar field  $\sigma(\zeta)$  are observed to be  $-58.39$  ( $-96.89$ ),  $-60.33$  ( $-97.32$ ),  $-63.11$  ( $-97.96$ ) and  $-64.38$  ( $-98.26$ ) MeV at temperatures  $T = 0, 50, 100$  and  $150$  MeV, respectively. When the strength of magnetic field is increased to  $eB = 8m_\pi^2$ , these are modified to  $-49.04$ ( $-95.02$ ),  $-51.97$ ( $-95.57$ ),  $-56.42$ ( $-96.47$ ) and  $-40.44$ ( $-93.59$ ) MeV, respectively. We observe that the percentage drop in the magnitude of scalar field  $\sigma(\zeta)$  is  $16.01\%$ ( $1.93\%$ ),  $13.86\%$ ( $1.80\%$ ),  $10.60\%$ ( $1.53\%$ ) and  $37.19\%$ ( $4.75\%$ ) at  $T=0, 50, 100$  and  $150$  MeV respectively. As can be seen, initially when temperature is increased from  $T = 0$  to  $100$  MeV, the value of the percentage drop decreases. However, at large value of temperature ( $T = 150$  MeV) and stronger magnetic field, the magnitudes of the scalar fields decrease much more rapidly with increasing magnetic field. This implies that for large value of temperature and stronger magnetic field, the inverse magnetic catalysis is observed in nuclear matter. This observation is also consistent with lattice QCD observations where the finite temperature and stronger magnetic field is observed to show the effect of inverse magnetic catalysis.

At zero temperature and for  $\rho_B = \rho_0$ , an increase in the value of isospin asymmetry parameter  $\eta$  from zero to finite value (say  $\eta = 0.3$ ) is observed to cause less drop in the magnitude of scalar field. As temperature is increased the impact of  $\eta$  is observed to weaken, i.e., values of scalar fields at finite  $\eta$  start approaching the values observed at  $\eta = 0$ . In nuclear medium, at sufficiently high  $T$  (for example at  $T = 150$  MeV) the drop in the value of scalar fields is observed to be more at  $\eta = 0.3$  as compared to  $\eta = 0$ . To quote in terms of numbers, we observe that for magnetic field  $eB = 8m_\pi^2$  and isospin asymmetry  $\eta = 0.3$ , the values of scalar fields  $\sigma(\zeta)$  are observed to be  $-52.02$ ( $-95.58$ ),  $-54.61$ ( $-96.09$ ),  $-59.03$ ( $-97.03$ ) and  $-37.96$ ( $-93.24$ ) MeV at temperature  $T = 0, 50, 100$  and  $150$  MeV. As can be seen, at  $T=150$  MeV, the magnitude of scalar fields at  $\eta = 0.3$  are observed to be smaller as compared to the values quoted earlier for  $\eta = 0$  case. This implies that at high temperatures and for strong magnetic fields, inverse magnetic catalysis is more favored in asymmetric nuclear matter as compared to symmetric nuclear matter, although the effect is small. It may be noted that the anomalous magnetic moments of nucleons are observed to affect the behavior of scalar fields more significantly in presence of finite Dirac sea as compared to when Dirac sea contributions are ignored. In the absence of the Dirac sea

contributions, but accounting for the finite anomalous magnetic moments of the baryons, the magnitude of scalar field increases with increasing the strength of magnetic field, at low and moderate temperature which implies that the magnetic catalysis effect is observed. However, at high temperature such  $T = 150$  MeV, the magnitude of scalar fields is observed to decrease with increase in the strength of magnetic field. It is observed that the impact of magnetic field is much more appreciable in presence of finite Dirac sea contributions, and the effect is particularly significant for stronger magnetic field and high temperature case.

We next study the effects of finite strangeness fraction on the behaviour of the scalar fields ( $\sigma$ ,  $\zeta$  and  $\delta$ ). At  $\rho_B = \rho_0$ , the inclusion of hyperons along with nucleons significantly alters the behaviour of scalar fields as a function of magnetic field, when the contributions due to the baryonic Dirac sea is taken into account. The solutions of the scalar fields exist upto  $eB \sim 5m_\pi^2$ , in the strange hadronic matter ( $f_s=0.3$ ) when the Dirac sea contributions and the AMMs of the baryons are taken into account. For  $\rho_B = 0$ , the scalar fields, which have solutions for values of  $eB$  upto  $4(2.8)m_\pi^2$ , when the Dirac sea contributions of the nucleons (and hyperons) are taken into account, along with the results when the DS effects are not considered, are plotted in figures 1 and 2. The non-existence of the solutions above a critical value of the magnetic field can be understood in the following way. For vacuum ( $\rho_B = 0, T=0$ ) of nuclear matter, the total scalar densities of the nucleons are solely due to contributions of the Dirac sea, and, the effective mass,  $m_i^*$  satisfies the equation

$$m_i^* - m_i = C_i \left[ \frac{(q_i B)^2}{3m_i^*} + \{(\kappa_i B)^2 m_i^* + (|q_i| B)(\kappa_i B)\} \left( \frac{1}{2} + 2 \ln \left( \frac{m_i^*}{m_i} \right) \right) \right]. \quad (54)$$

where  $C_i = A_i/(4\pi^2)$ , with  $A_i$  defined in equation (31). In the simplifying assumption of neglecting the logarithm term in the last term on the right hand side of the above equation,  $m_i^*$  satisfies the quadratic equation

$$(1 - C_i(\kappa_i B)^2)m_i^{*2} - \left( m_i + \frac{C_i |q_i B| (\kappa_i B)}{2} \right) m_i^* - \frac{C_i (q_i B)^2}{3} = 0. \quad (55)$$

For real solutions for  $m_i^*$ , we should have  $\left( m_i + \frac{C_i |q_i B| (\kappa_i B)}{2} \right)^2 \geq \frac{4}{3}(1 - C_i(\kappa_i B)^2)C_i(q_i B)^2$ . Also, for  $C_i(\kappa_i B)^2 \geq 1$ , i.e., for the value of the magnetic field above a critical value of  $B_{crit} \sim 1/(C_i \kappa_i^2)^{1/2}$ , the above equation does not have a positive solution for  $m_i^*$ , both for the charged ( $q_i \neq 0$ ) and neutral ( $q_i = 0$ ) baryons. It might be noted that the above equation corresponds to the case when there are no meson-meson interaction terms for the scalar fields in the Lagrangian. In the presence of these quartic interaction terms (as given by equation

(7)) in the chiral model, the effective masses of the baryons,  $m_i^*(= -g_{\sigma i}\sigma - g_{\zeta i}\zeta - g_{\delta i}\delta)$ , are obtained from the scalar fields, which are solved, along with the dilaton field,  $\chi$  and the vector fields, from their coupled equations of motion given by equations (19) – (25). In the absence of hyperons, the scalar densities of nucleons, for  $\rho_B = 0$ , are solely due to the negative contributions of the Dirac sea, which leads to an increase in the magnitudes of the scalar fields (hence an enhancement of the light quark condensates) with increase in the strength of the magnetic field. This effect of magnetic catalysis for  $\rho_B = 0$  is observed, for both the cases of without and with the effects from the nucleon anomalous magnetic moments (AMMs) [33, 34, 59, 62, 63]. In the present investigation of strange hadronic matter at finite temperatures in the presence of a magnetic field, for  $f_s=0.3$  and  $\rho_B = \rho_0$ , the number densities for the hyperons remain negligible (except for  $\Xi^-$ ) and hence the contributions to the total scalar densities of these hyperons turn out to be negative, solely due to the contributions from the Dirac sea, as given by equation (32). It is observed that the solutions for the scalar fields do not exist for values of the magnetic field above a critical value ( $eB_{crit} \sim 5m_\pi^2$  for  $f_s = 0.3$  and  $\eta=0.3$ ), similar to the situation of the vacuum in nuclear matter, for reasons described above. Also, as the magnetic field is raised, for the hyperons, which are absent for  $\rho_B = \rho_0$ , the total scalar densities are negative, solely due to the Dirac sea contributions, leading to an increase in the magnitudes of scalar fields ( $\sigma$  and  $\zeta$ ), leading to magnetic catalysis effect in the magnetized strange hadronic matter (with  $f_s = 0.3$ ), contrary to the opposite behaviour of the scalar fields (hence of the light quark condensate) with magnetic field for the nuclear matter at  $\rho_B = \rho_0$ , when the AMMs of the baryons are taken into account. In the presence of Dirac sea contributions from the nucleons (hyperons along with nucleons), the effect of magnetic catalysis (an increase in the magnitude of scalar fields with increasing magnetic field strength) is observed for  $\rho_B = 0$ , as might be seen from figures 1 and 2.

In figures 3 and 4, the masses of the  $D(D^0, D^+)$  mesons are plotted as functions of  $eB/m_\pi^2$  for the magnetized asymmetric matter (with  $\eta=0.3$ ) at nuclear matter saturation density ( $\rho_B = \rho_0$ ) for the nuclear ( $f_s=0$ ) and hyperonic matter (with  $f_s=0.3$ ) respectively. In the left panel of these figures, results for the mass modifications of  $D$  mesons are also shown at  $\rho_B = 0$ , considering magnetized Dirac sea of nucleons and in the right panel, due to both the nucleons as well as hyperons. The anomalous magnetic moments (AMMs) of the baryons are taken into account in the present study. The  $D^+$  and  $D^0$  masses are shown for

values of the temperature  $T=50, 100$  and  $150$  MeV. The in-medium behaviors of the scalar fields are reflected in the medium modification of  $D$  meson properties. The lowest Landau level (LLL) contribution is taken into account for the charged  $D^+$  meson. At finite baryon density, in the absence of Dirac sea contributions, when the PV mixing is not taken into account, one observes the mass of the neutral  $D$  meson to be insensitive to the variation in the magnetic field whereas  $D^+$  mass shows a steady increase due to the LLL contributions. Including the Dirac sea contributions and the anomalous magnetic moments of nucleons, initially the in-medium mass of  $D^+$  meson is seen to increase with magnetic field upto a certain value and then starts decreasing with further increase in  $eB$ . The drop in the mass at higher values of magnetic field is observed to be sharper as the temperature is raised from  $T=50$  MeV to  $T=100$  and  $150$  MeV. In the presence of PV ( $D - D^*$ ) mixing, there is seen to be a drop in the mass of both the  $D^+$  and  $D^0$  mesons, which is observed to be much more pronounced for the neutral  $D$  meson. The effect of the isospin asymmetry is observed to be small. For example, for  $\rho_B = \rho_0$  and  $f_s = 0$  the value of the  $D^+(D^0)$  mass (in MeV) is observed to be 1736.5 (1585.9) for  $eB = 10m_\pi^2$  for  $T=50$  MeV and 1615.86 (1416.3) at  $T=150$  MeV for the same value of the magnetic field for  $\eta=0.3$ , when the Dirac sea as well as PV mixing are taken into account, in addition to LLL contribution for  $D^+$  meson, which may be compared to the  $\eta=0$  values of 1732.85 (1554.5) and 1625.6 (1414.9) at  $T=50$  and  $T=150$  MeV respectively. Thus the isospin asymmetry effect is small, but larger for neutral  $D$  meson at smaller temperature of  $T=50$  MeV, whereas, for  $D^+$  mass, the effect of isospin asymmetry is observed to be marginal.

The effect of strangeness is shown in figure 4, which shows the magnetic field dependence of the  $D$  meson masses for the asymmetric ( $\eta = 0.3$ ) hyperonic matter (with  $f_s=0.3$ ) for  $\rho_B = \rho_0$ . Similar to the case of asymmetric (with  $\eta=0.3$ ) nuclear matter ( $f_s=0$ ) as shown in figure 3, in the absence of the Dirac sea contributions, the  $D^0$  mass is observed to be insensitive to the variation in the magnetic field, whereas the LLL contribution leads to a monotonic increase in the mass of  $D^+$  mesons with  $eB$ , when the PV ( $D - D^*$ ) mixing is not taken into account. The PV mixing leads to a drop in the masses of both  $D^+$  and  $D^0$ , with a much larger decrease for  $D^0$  mass, as has been observed for the case of magnetized nuclear matter ( $f_s=0$ ). At  $\rho_B = \rho_0$ , in the presence of the Dirac sea contributions, the solutions for the scalar fields exist only upto a value of  $eB = 5m_\pi^2$ , as has already been mentioned. There is observed to be an increase in the mass of  $D^+$  as was observed for

$f_s=0$  case upto  $eB = 5m_\pi^2$ . For zero magnetic field, when the strangeness fraction  $f_s$  is changed from 0 to 0.3, the value of the mass of  $D^+$  ( $D^0$ ) is modified from 1797.9 (1792.2) to 1791 (1799.8) for  $T=50$  MeV, and 1801.86 (1798.1) to 1794.8 (1803.9) for  $T=150$  MeV. For  $eB = 5m_\pi^2$ , the modifications in the masses due to increase in  $\eta$  from 0 to 0.3 are 1857 (1788.4) to 1855.7 (1801.8) and 1884.5 (1816.5) to 1882.1 (1826.1) for  $T=50$  and  $T=150$  MeV respectively. The effects of the isospin asymmetry on the  $D^+$  and  $D^0$  meson masses for the strange hadronic matter are thus observed to be similar to the symmetric case. As has already been mentioned, at zero baryon density, in the presence of magnetized Dirac sea of nucleons (nucleons and hyperons), the solutions of scalar fields exist upto  $eB \sim 4(2.8)m_\pi^2$ . The  $D$  mesons masses for  $\rho_B = 0$  with the Dirac sea contributions are plotted upto these values of magnetic field in figures 3 and 4. The LLL contribution (for the charged  $D^+$  meson) causes an increase in the mass as a function of magnetic field both at zero baryon density as well as at  $\rho_B = \rho_0$ , whereas the mass decreases due to the PV mixing. At zero baryon density, the effects of Dirac sea contributions due to nucleons (nucleon and hyperons) on the in-medium masses of the  $D^+$  and  $D^0$  mesons are observed to be marginal as compared to when these effects are ignored, upto a value of  $eB$  around  $3.5(2)m_\pi^2$  beyond which there is observed to be a drop with further increase in the magnetic field.

The dependence of in-medium masses of  $D^-$  and  $\bar{D}^0$  mesons on the magnetic field are shown in figures 5 and 6 for values of the isospin asymmetry parameter  $\eta = 0.3$ , for magnetized nuclear ( $f_s = 0$ ) and hyperonic (with  $f_s=0.3$ ) matter respectively, at  $\rho_B = \rho_0$ , along with the results for zero baryon density. At  $\rho_B = \rho_0$ , in magnetized nuclear matter ( $f_s=0$ ), for a given magnetic field strength, the in-medium masses of  $\bar{D}$  mesons are observed to be larger than the masses of the  $D$  mesons. However, the trend of variation of in-medium masses of  $\bar{D}$  mesons as functions of the magnetic field are found to be similar to those of the  $D$  mesons. The effects of the isospin asymmetry of the nuclear medium on the masses of the  $\bar{D}$  mesons are observed to be small compared to the effects from the Dirac sea and PV mixing effects, similar to what was observed for the  $D$  mesons. As has already been mentioned, at finite strangeness fraction with  $f_s = 0.3$  and  $\rho_B = \rho_0$ , the solutions for the scalar fields exist only upto  $eB = 5m_\pi^2$ , when the Dirac sea contributions are considered by summing over the tadpole diagrams in the weak magnetic field limit. Similar to the mass of the  $D$  meson, the  $\bar{D}$  meson masses are observed to increase with magnetic field upto  $5m_\pi^2$ . As has been observed for the  $D$  mesons, the masses of  $\bar{D}$  mesons have very small effect

from the isospin asymmetry for the nuclear as well as hyperonic matter. For  $\rho_B = 0$ , the behaviour of  $\bar{D}$  masses are observed to be similar to the masses of the  $D$  mesons.

At finite density, the dominant magnetic field effects on the  $D$  and  $\bar{D}$  mesons are due to the Dirac sea and PV mixing and the effects of isospin asymmetry are observed to be marginal. The qualitative trends of the  $D$  and  $\bar{D}$  masses both for the nuclear and hyperonic matter are observed to be similar at temperatures ( $T=50, 100$  and  $150$  MeV) considered in the present study. However, in nuclear matter (both for  $\eta=0$  and  $0.3$ ), the masses of all these mesons are observed to initially increase followed by a drop, but the value of  $eB$  where the masses start decreasing, are observed to be smaller when the temperature is raised and the value is much smaller for  $T=150$  MeV.

The in-medium mass of charmonium state  $\psi(3770)$  as function of  $eB$  is shown in figure 7 for the asymmetric (with  $\eta=0.3$ ) nuclear matter ( $f_s=0$ ) and the hyperonic matter (with  $f_s=0.3$ ), at  $\rho_B = \rho_0$ , along with results for  $\rho_B = 0$ . At finite  $\rho_B$ , in the presence of Dirac sea contributions, in nuclear matter, both for symmetric and asymmetric cases, there is observed to be an increase in the mass followed by a drop with further increase in the magnetic field. However, similar to the cases of  $D$  and  $\bar{D}$  meson masses, the effects of isospin asymmetry are observed to be small for the charmonium ( $\psi(3770)$ ) mass. The value of  $eB$  for which the behaviour changes from an increase in mass to a drop, is observed to be smaller when the temperature is raised. As has been already mentioned, the masses of the charmonium states are obtained from the medium change of the gluon condensate and also depend on the wave function of the particular state considered, using equation (40). The contribution from PV mixing leads to a negative (positive) contribution to the mass of the pseudoscalar (longitudinal component of the vector) meson. This is calculated from the phenomenological Lagrangian corresponding to the process  $V \rightarrow P\gamma$ . For  $T=150$  MeV, the mass of the  $\psi(3770) \equiv \psi(1D)$  turns out to be smaller than the mass of  $\eta'_c \equiv \eta_c(2S)$  for  $eB$  larger than around  $8.5 m_\pi^2$ , due to which the process  $\psi(3770) \rightarrow \eta'_c\gamma$  is no longer kinematically possible. The effect due to PV mixing on the mass of  $\psi(3770)$  exist upto  $eB = 8.5m_\pi^2$  for  $T=150$  MeV, for symmetric and asymmetric nuclear matter. These can be seen from panel (e) of figure 7 for asymmetric nuclear matter. At  $\rho_B = \rho_0$ , in the presence of strangeness fraction, including the Dirac sea contributions, lead to solutions for the mass of  $\psi(3770)$  upto  $eB = 5m_\pi^2$ , which is observed to increase with the magnetic field for the temperatures  $T=50, 100$  and  $150$  MeV, both for isospin symmetric and asymmetric

cases. This can be observed from panels (b), (d) and (f) for asymmetric hyperonic matter in figure 7. At zero baryon density, with magnetized Dirac sea of nucleons (and hyperons), the effective masses of charmonium state (calculated from the medium change of the dilaton field) are obtained upto  $4(2.8)m_\pi^2$ , due to non-existence of solutions of scalar fields above these values of magnetic field. The DS effects are observed to be marginal for  $eB$  upto around  $3.5(2)m_\pi^2$  above which there is observed to be a drop in the charmonium mass.

Figure 8 shows the dependence of the partial decay width of  $\psi(3770) \rightarrow D\bar{D}$ , along with the contributions from the subchannels (I)  $\psi(3770) \rightarrow D^+D^-$  and (II)  $\psi(3770) \rightarrow D^0\bar{D}^0$ , computed using the  $^3P_0$  model. These decay widths are shown for magnetized matter for  $\rho_B = 0$  and also for asymmetric (with  $\eta=0.3$ ) nuclear as well as hyperonic matter (with  $f_s=0.3$ ) at  $\rho_B = \rho_0$  and for values of temperature as 50, 100 and 150 MeV. The medium modifications of the decay widths arise due to the medium modifications of the masses of the initial and final states as calculated using the chiral model including the effects of the baryonic Dirac sea, with additional contributions from PV mixing as well as the lowest Landau level (LLL) for the charged open charm mesons. The effects due to the PV mixing ( $\psi(3770) - \eta'_c$ ,  $D - D^*$  and  $\bar{D} - \bar{D}^*$ ) are considered. These decay widths are compared with the values when the Dirac sea effects are not considered. When the PV mixing effects are not taken into account, the decay width of  $\psi(3770)$  to  $D^0\bar{D}^0$  remains insensitive to the change in the magnetic field when the Dirac sea contributions are not considered as the masses are almost unaffected by the magnetic field for the neutral open charm mesons [47] and the charmonium state [49]. However, in the absence of Dirac sea effects, the decay width to the charged  $D\bar{D}$  final state is observed to decrease with increase in the magnetic field and vanish as the magnetic field is further increased, when the PV mixing effects are still not considered [50]. This is due to LLL contributions which leads to a rise in the masses of the charged open charm mesons [47]. The incorporation of the PV mixing effects (due to  $\psi(3770) - \eta'_c$ ,  $D(\bar{D}) - D^*(\bar{D}^*)$ ) is observed to lead to significant modifications to the decay widths of  $\psi(3770)$  to the charged and neutral  $D\bar{D}$  due to the magnetic field, both for nuclear and strange hadronic matter. Accounting for the PV mixing, but when the Dirac sea (DS) effects of the baryons are not taken into consideration, within the  $^3P_0$  model, there is observed to be an initial slow decrease in the decay width for the charged  $D\bar{D}$  mesons channel with the increase in the magnetic field, which remains almost constant at higher values of the magnetic field, whereas, the neutral  $D\bar{D}$  channel shows an initial increase followed by a



drop with further increase in the value of the magnetic field. This behaviour is observed for symmetric as well as asymmetric (with  $\eta=0.3$ ) for both nuclear matter and hyperonic matter. This can be seen from figure 8, plotted for asymmetric nuclear and hyperonic matter. In the presence of Dirac sea contributions, the behaviour of the decay widths with magnetic field remain similar and the effects from PV mixing are observed to dominate over the effects of Dirac sea. The decay widths, obtained upto  $eB \sim 4(2.8)m_\pi^2$  with the effects of Dirac sea of the nucleons (and hyperons) for  $\rho_B = 0$ , have similar trend as for  $\rho_B = \rho_0$ .

The magnetic field dependence of the charmonium decay widths are shown for asymmetric nuclear and hyperonic matter in figure 9 using the field theoretical (FT) model of composite hadrons. At  $\rho_B = \rho_0$ , the decay width in asymmetric nuclear matter in the charged  $D\bar{D}$  channel is observed to decrease with the magnetic field upto  $eB \sim 6m_\pi^2$ , beyond which there is observed to be a slow increase. The values of the decay width (in MeV) are observed to be 31.48, 19.12 and 24.86 for values of  $eB$  (in units of  $m_\pi^2$ ) as 0, 6 and 10 respectively for  $T=50$  MeV when the DS effects are taken into account. On the other hand, the decay width for the neutral  $D\bar{D}$  channel is observed to have a substantial increase with the magnetic field, from the value of 22.68 MeV at  $eB = 0$  reaching a maximum of around 78.3 MeV for  $eB \sim 7.5m_\pi^2$ , for the same temperature, beyond which there is observed to be a slow drop as the magnetic field is further increased. This leads to the maximum value of the total decay width to be 98.9 MeV for  $eB = 8.5m_\pi^2$  for  $T=50$  MeV in asymmetric nuclear matter when the DS effects are taken into account. Similar behaviours of the decay widths are observed for the temperatures  $T=100$  and  $150$  MeV for asymmetric nuclear matter. The Dirac sea (DS) contributions are observed to lead to smaller values of decay width, although the changes due to DS effects are marginal. In the presence of hyperons in the medium, the decay widths follow similar trend as for the nuclear matter for  $T=50, 100$  and  $150$  MeV, as can be observed from figure 9. At  $\rho_B = \rho_0$ , the decay widths are plotted only upto  $eB = 5m_\pi^2$  for strange hadronic matter, when the DS effects are taken into account since the solutions for the scalar fields do not exist for  $eB$  larger than  $5m_\pi^2$ , as has already been mentioned. In figure 9, the decay widths of  $\psi(3770)$  to charged and neutral  $D\bar{D}$  mesons, along with the total of both subchannels, obtained using the field theoretical model, are also plotted for  $\rho_B = 0$ , and, are observed to have similar trend as obtained using the  ${}^3P_0$  model. The magnetic field effect on the decay width due to PV mixing is observed to dominate over the effect from Dirac sea within the  ${}^3P_0$  model as well as the field theoretical (FT) model of

composite hadrons.

The production cross-sections of  $\psi(3770)$ , arising from the scattering of (I)  $D^+D^-$  and (II)  $D^0\bar{D}^0$  mesons are plotted as functions of the invariant mass for magnetized asymmetric (with  $\eta=0.3$ ) nuclear ( $f_s=0$ ) and hyperonic (with  $f_s=0.3$ ) matter with  $\psi(3770) \rightarrow D^+D^-(D^0\bar{D}^0)$  decay width computed using the  $^3P_0$  model in figures 10 and 11 and using FT model, in figures 12 and 13, at  $\rho_B = \rho_0$  for  $T=50, 100$  and  $150$  MeV. These are plotted for values of  $eB = 2.5m_\pi^2$  and  $eB = 8m_\pi^2$ . For  $\rho_B = 0$ , for which the results for the production cross-sections with the Dirac sea effects due to the nucleons (and hyperons) exist for  $eB$  upto around  $4(2.8)m_\pi^2$ , the production cross-sections are shown for  $eB = 2.5m_\pi^2$  (left panels of Figs. 10 –13). The PV ( $\psi(3770) - \eta'_c$ ) mixing modifies the mass of the longitudinal component of the charmonium state,  $\psi(3770)$ , whereas, the transverse components remain unaffected due to PV mixing. There is observed to be well-separated distinct peak positions in the production cross-sections of  $\psi(3770)$  due to scattering of (I)  $D^+D^-$  and (II)  $D^0\bar{D}^0$  plotted as functions of the invariant mass, for the higher value of the magnetic field ( $eB = 8m_\pi^2$ ), as the PV mixing effects are more dominant with increase in the magnetic field. For magnetized asymmetric (with  $\eta=0.3$ ) nuclear matter, at  $\rho_B = \rho_0$ , and for the values of temperatures of  $T=50, 100$  and  $150$  MeV respectively, the production cross-sections due to the scattering of the  $D^+D^-$  and  $D^0\bar{D}^0$  are plotted as functions of the invariant mass in panels (a), (c), and (e) for  $eB = 2.5m_\pi^2$  and in panels (b), (d) and (f) for  $eB = 8m_\pi^2$  in figure 10. For  $D^+D^-(D^0\bar{D}^0)$  channel, these are observed to be maximum at positions (in MeV) of 3706 (3706), 3722 (3722) and 3726 (3726) when the Dirac sea (DS) effects are taken into account, and 3708 (3708), 3724 (3722) and 3728 (3728), when these are not taken into consideration. It might be noted here that the production cross-section due to scattering of  $D^+D^-$  as well as  $D^0\bar{D}^0$  has contributions due to the transverse and longitudinal components of  $\psi(3770)$ , which have different masses due to PV mixing. The masses (in MeV) of the longitudinal (transverse) component of  $\psi(3770)$  for  $\rho_B = \rho_0$ ,  $f_s = 0$  and  $\eta = 0.3$  and  $T=50, 100$  and  $150$  MeV, are observed to be 3723.6 (3703.4), 3745.8 (3719.2) and 3744.1 (3725), in the presence of DS effects, and, 3725 (3705), 3740 (3720.7) and 3725 (3751), when the DS effects are neglected. It is thus observed that the production cross-sections of  $\psi(3770)$  due to scattering of the charged as well as neutral  $D\bar{D}$  are peaked at position close to the transverse mass of  $\psi(3770)$ , for  $eB = 2.5m_\pi^2$ . At  $\rho_B = \rho_0$ , the production cross-sections of  $\psi(3770)$  due to the scatterings of (I)  $D^+D^-$  and (II)  $D^0\bar{D}^0$  mesons are observed to be

very similar for the magnetic field  $eB = 2.5m_\pi^2$ , with the value of the peak height to be marginally larger for the channel (I)  $D^+D^-$  as compared to (II)  $D^0\bar{D}^0$ , as might be seen from panels (a), (c) and (e) for  $T=50, 100$  and  $150$  MeV. However, both with as well as without DS effects, for  $\rho_B = 0$  and  $eB = 2.5m_\pi^2$ , the peak height is observed to be much larger for the  $D^0\bar{D}^0$  as compared to the value for  $D^+D^-$  scattering. E.g., the value of the peak height is  $82.5\text{mb}$  for  $D^0\bar{D}^0$  is much larger as compared to the value of  $59.8\text{mb}$  for  $D^+D^-$  scattering, for  $T=50$  MeV, in the presence of DS effects. The effect of temperature on the production cross-sections is observed to be very small for  $eB = 2.5m_\pi^2$ . At the higher magnetic field of  $eB = 8m_\pi^2$ , the masses with and without PV mixing are quite different, as can be seen from figure 7, with the values of  $3644.4$  ( $3774.26$ ),  $3682.9$  ( $3806.65$ ) and  $3442$  ( $3608.9$ ) MeV for  $T=50, 100$  and  $150$  MeV respectively, when the Dirac sea (DS) effects are taken into account, and at  $3708.25$  ( $3828.1$ ),  $3721.6$  ( $3839.1$ ) and  $3702.2$  ( $3823$ ) MeV when these are not taken into consideration. The masses (in MeV) of the longitudinal (transverse) component of  $\psi(3770)$  for  $\rho_B = \rho_0$ ,  $f_s = 0$ ,  $\eta = 0.3$ ,  $eB = 8m_\pi^2$ , and  $T=50, 100$  and  $150$  MeV, are observed to be  $3774.3$  ( $3644.4$ ),  $3806.7$  ( $3682.9$ ) and  $3608.9$  ( $3442$ ), in the presence of DS effects, and,  $3828.1$  ( $3708.2$ ),  $3839.1$  ( $3721$ ) and  $3823$  ( $3702$ ), when the DS effects are neglected. For the higher value of the magnetic field,  $eB = 8m_\pi^2$ , as can be seen from panels (b), (d) and (f) in figure 10 for temperatures  $T=50, 100$  and  $150$  MeV respectively, the larger mass difference in the transverse and longitudinal components of  $\psi(3770)$  leads to the peaks to be well separated, both for  $\rho_B = \rho_0$  as well as for  $\rho_B=0$ . The positions of the peaks are observed to be close to the longitudinal (transverse) mass of  $\psi(3770)$ , due to the scattering of  $D^+D^-$  ( $D^0\bar{D}^0$ ) mesons. The production cross-sections from the  $D^+D^-$  scattering is observed to have additional peaks at positions close to the transverse (lower) mass of  $\psi(3770)$  for  $T=50$  and  $100$  MeV for  $\rho_B = \rho_0$  (with  $\eta=0.3$ ,  $f_s=0$ ), in the absence of the Dirac sea effects, as can be seen from panels (b) and (d) (as the widely-spaced dotted lines) of Fig. 10. It is observed that the individual production cross-sections are diminished for the higher value of the magnetic field,  $eB = 8m_\pi^2$ , with the heights of the peaks (in mb) to be given as  $17.62$  ( $17.57$ ) and  $26.12$  ( $25.56$ ) for  $T=50$  ( $100$ ) MeV and  $\rho_B = \rho_0$ , due to channels (I) and (II) respectively, in the presence of DS effects, as compared to the values of the heights to be  $55.39$  ( $54.85$ ) and  $54.15$  ( $52.91$ ) for  $eB = 2.5m_\pi^2$ . At  $\rho_B = \rho_0$ , for  $T=150$  MeV and  $eB = 8m_\pi^2$ , with DS effects, the peak heights (in mb) are observed to be  $23.26$  and  $19.49$  for channels (I) and (II) respectively, which are similar to the values of  $24.52$  and

18.94 to the case when DS effects are not taken into account.

In the presence of hyperons in the medium, when the Dirac sea effects are taken into account, there is observed to be an increase in the mass of charmonium state  $\psi(3770)$  as calculated within the chiral effective model using equation (40), whose longitudinal component has a further positive shift due to the PV mixing, for  $T=50, 100$  and  $150$  MeV, as can be seen for asymmetric ( $\eta=0.3$ ) strange ( $f_s=0.3$ ) hadronic matter in figure 7. The behaviour of the charmonium mass is reflected in the peak positions of the production cross-section as plotted for the magnetized asymmetric strange hadronic matter in figure 11. The production cross-sections of  $\psi(3770)$  are plotted in figure 11 for asymmetric (with  $\eta=0.3$ ) strange (with  $f_s=0.3$ ) hadronic matter for  $eB = 2.5m_\pi^2$  and  $eB = 8m_\pi^2$ , for  $T=50, 100$  and  $150$  MeV and  $\rho_B = \rho_0$  (also, at  $\rho_B = 0$  for  $eB = 2.5m_\pi^2$ ). For  $eB = 2.5m_\pi^2$ , the behaviour of the production cross-sections in the channels (I) and (II) are observed to be similar to the case of asymmetric nuclear matter (shown in panels (a), (c) and (e) in figure 10). However, the peak positions are shifted to higher values when the DS effects are taken into consideration as compared to when the Dirac sea of the baryons are ignored. At  $\rho_B = \rho_0$  and  $eB = 2.5m_\pi^2$ , the DS effects are observed to be larger as compared to the magnetized nuclear matter shown in figure 10. As has already been mentioned, at  $\rho_B = \rho_0$ , for  $eB$  higher than  $5m_\pi^2$ , the solutions for the scalar fields do not exist for the strange hadronic matter, when the Dirac sea effects of baryons are taken into account in the weak magnetic field limit as used for the computation of the baryon self-energy accounting for the magnetized Dirac sea [34]. The dependence of the production cross-sections on the invariant mass are observed to be similar to the case of magnetized nuclear matter for the higher value of the magnetic field,  $eB = 8m_\pi^2$ , when the Dirac sea effects are not taken into account.

The production cross-sections of  $\psi(3770)$  are plotted for magnetized asymmetric (with  $\eta=0.3$ ) nuclear ( $f_s=0$ ) and hyperonic (with  $f_s=0.3$ ) matter in figures 12 and 13 using FT model, for values of  $eB = 2.5m_\pi^2$  and  $eB = 8m_\pi^2$ . The larger values of the charmonium decay width obtained using the field theoretical (FT) model as compared to the values calculated within the  ${}^3P_0$  model are observed as a broadening of the peaks in the invariant mass plot of the production cross-section of  $\psi(3770)$ . The effects from the temperature and strangeness are observed to be significant in the present study of the production cross-section of the charmonium state  $\psi(3770)$  for higher values of the magnetic field, which are obtained from the in-medium mass and decay widths of the charmonium state in the

magnetized nuclear (hyperonic) matter. The PV mixing effect is observed to dominate over the Dirac sea effect. In the invariant mass plot of production cross-sections of  $\psi(3770)$  the production cross-sections for the scatterings from (I)  $D^+D^-$  and (II)  $D^0\bar{D}^0$  are observed to be peaked at the positions close to the mass of the longitudinal and transverse components of the charmonium state  $\psi(3770)$  for higher values of the magnetic field ( $eB = 8m_\pi^2$ ) for magnetized nuclear matter, when the DS effects are taken into consideration for  $\rho_B = \rho_0$ , as well as, for  $\rho_B=0$ , when the Dirac sea effects are not taken into account. In the absence of DS effects, for  $eB = 8m_\pi^2$ , both for the nuclear and hyperonic matter, additional peaks are observed for  $T=50$  and  $100$  MeV for the production cross-section of the charmonium state in the charged  $D\bar{D}$  channel, close to the transverse mass of  $\psi(3770)$  at  $\rho_B = \rho_0$ , as can be seen from panels (b) and (d) of figures 10–13. For  $T=150$  MeV, the peaks are observed to be appreciably well-separated as compared to the lower temperatures ( $T=50$  and  $100$  MeV). The production cross-sections of  $\psi(3770)$  can have consequences on the dilepton spectra as well as the production of the charmonium as well as open charm mesons produced in ultra-peripheral ultra-relativistic heavy ion collision experiments, since the magnetic field created in these collisions are extremely large and the charm mesons are created at the early stage of the collision.

## V. SUMMARY

To summarize, in the present paper, we have investigated the charmonium production cross-sections due to scatterings of  $D^+D^-$  ( $D^0\bar{D}^0$ ) mesons, in the presence of an external magnetic field at finite temperatures, for  $\rho_B = 0$  as well as in isospin asymmetric nuclear (hyperonic) matter for  $\rho_B = \rho_0$ . In the peripheral ultra-relativistic heavy ion collisions, strong magnetic fields are produced. However, since the created matter has extremely low density, we investigate the production cross-sections of the charmonium state,  $\psi(3770)$ , which is the lowest state which decays to  $D\bar{D}$  in vacuum. The production cross-sections are calculated from the Breit-Wigner spectral function of the charmonium state, which is expressed in terms of its in-medium mass and decay width. The effects of Dirac sea as well as PV mixing, in addition to the lowest Landau level (LLL) contributions for the charged mesons, are taken into consideration to calculate the masses of the open charm ( $D$  and  $\bar{D}$ ) mesons and the charmonium state  $\psi(3770)$  and the subsequent effect on the partial decay

width of  $\psi(3770) \rightarrow D\bar{D}$  in magnetized isospin asymmetric nuclear (hyperonic) matter for  $\rho_B = \rho_0$  as well as for  $\rho_B = 0$ , at finite temperatures. The decay widths are calculated using two light quark-antiquark models: (I) the  $^3P_0$  model and (II) a field theoretical (FT) model of composite hadrons, and their effects on the production cross-section of  $\psi(3770)$  are studied in the present work.

Within a chiral effective model, the in-medium masses of the open charm mesons are calculated from their interactions with the scalar (isoscalar  $\sigma$  and isovector  $\delta$ ) mesons and the baryons, whereas the mass modification of the charmonium state  $\psi(3770)$  is obtained from the medium change of a dilaton field, which simulates the gluon condensates of QCD. The anomalous magnetic moments (AMMs) of the baryons are taken into consideration in the present work. At finite baryon density, accounting for the Dirac sea effects and the AMMs of the baryons, we observe the inverse magnetic catalysis (drop in the magnitude of the scalar fields  $\sigma$  and  $\zeta$ , which are proportional to the strengths of the light non-strange and strange quark condensates, with increase in the magnetic field) in magnetized nuclear matter, contrary to the opposite effect of magnetic catalysis (MC) at zero baryon density. The inclusion of the hyperons to the nuclear matter at finite baryon density is observed to lead to the effect of magnetic catalysis. The effect of (inverse) magnetic catalysis is observed to be enhanced with the increase in the temperature. In the absence of the Dirac sea effects, the scalar fields ( $\sigma$  and  $\zeta$ ) are observed to remain almost unaffected when the magnetic field is increased for temperatures  $T=50$  and  $100$  MeV, whereas, there is observed to be a rise with  $eB$  for  $T=150$  MeV, both for the nuclear and hyperonic matter at  $\rho_B = \rho_0$ . The effect due to the isospin asymmetry is observed to be marginal as compared to the Dirac sea effects. In the absence of Dirac sea as well as PV contributions, the neutral open charm meson masses are observed to be insensitive to the variation of the magnetic field within the chiral model, whereas, the masses of the charged  $D^\pm$  mesons have positive contributions from the lowest Landau level (LLL) leading to a monotonic increase as magnetic field is raised. At finite density, the PV mixing effects of the open charm mesons ( $D - D^*$  and  $\bar{D} - \bar{D}^*$  mixings) are observed to lead to drop in the masses of the pseudoscalar open charm ( $D$  and  $\bar{D}$ ) mesons. The Dirac sea effects in nuclear matter for  $\rho_B = \rho_0$  are observed to lead to an initial increase with increase in the magnetic field, followed by a drop of the open charm meson masses and the value for which it starts decreasing is smaller with increase in the temperature. In hyperonic matter, at  $\rho_B = \rho_0$ , the masses are observed to lead to an

increase upto  $eB \sim 5m_\pi^2$ , upto which the solutions for the scalar fields can be found using the weak magnetic field approximation for obtaining the baryon self energy incorporating the Dirac sea contributions by summing over the tadpole diagrams.

The  $\psi(3770)$  mass is observed to show a similar trend as for the open charm mesons, when the Dirac effects are considered. The mass of the longitudinal component of  $\psi(3770)$ , is observed to increase due to the mixing with pseudoscalar meson,  $\eta'_c$ . Due to PV mixing, the production cross-section of  $\psi(3770)$ , arising due to the scatterings of (I)  $D^+D^-$  and (II)  $D^0\bar{D}^0$  mesons, are observed to have distinct peak positions in the invariant mass spectrum for the higher value of the magnetic field,  $eB = 8m_\pi^2$ , in the magnetized nuclear (hyperonic) matter for  $\rho_B = \rho_0$  as well as for  $\rho_B = 0$ . This arises due to the difference in the masses of the longitudinal and transverse components, since the former is modified, whereas, the transverse component is unaffected by PV mixing. In the presence of DS effects of the baryons, for  $eB = 8m_\pi^2$ , it is observed that the production cross-sections of  $\psi(3770)$  due to scatterings of (I)  $D^+D^-$  and (II)  $D^0\bar{D}^0$  mesons are peaked at the positions close to the masses of the longitudinal and transverse components of  $\psi(3770)$  respectively. In the absence of the Dirac sea contributions, there are observed to be additional peaks for the charmonium cross-section arising from  $D^+D^-$  scattering, at the positions close to the transverse mass of the charmonium state. For  $\rho_B = 0$  and  $eB = 2.5m_\pi^2$ , the peak height is observed to be much larger for the  $D^0\bar{D}^0$  as compared to the value for  $D^+D^-$  scattering, with as well as without DS effects. The peak heights are observed to drop appreciably as the magnetic field is increased. There is observed to be appreciable increase in the separation between the peaks when the temperature is raised to 150 MeV. The charmonium decay widths calculated using the field theoretical (FT) model of composite hadrons are observed to be much larger than the values calculated using the  $^3P_0$  model, which is reflected in the production cross-sections of  $\psi(3770)$  as an appreciable broadening of the peaks. The present study of the charmonium production in isospin asymmetric strange hadronic matter at finite temperature and in presence of strong magnetic fields can have observational consequences on the production of the open and hidden charm mesons in asymmetric ultra-relativistic peripheral heavy ion collision experiments.

---

[1] T. Vachaspati, Phys. Lett. B **265**, 258 (1991).

- [2] R. Durrer and A. Neronov, *Astron. Astrophys. Rev.* **21**, 62 (2013).
- [3] D. E. Kharzeev et al., *Nucl. Phys. A* **803**, 227 (2008).
- [4] K. Fukushima et al., *Phys. Rev. D* **78**, 074033 (2008).
- [5] V. V. Skovov et al., *Int. J. Mod. Phys. A* **24**, 5925 (2009).
- [6] Roberto Turolla, Silvia Zane, Anna Watts, *Rept.Prog.Phys.* **78**, 116901 (2015).
- [7] Manisha Kumari and Arvind Kumar, *Int. J. Mod. Phys. E* **31**, 2250050 (2022).
- [8] Debraj Kundu, Vivek Baruah Thapa and Monika Sinha, *Phys. Rev. C* **107**, 035807 (2008).
- [9] V. P. Gusynin, V. A. Miransky, and I. A. Shovkovy, *Nucl. Phys. B* **462**, 249 (1996),
- [10] G. S. Bali, F. Bruckmann, G. Endrodi, Z. Fodor, S. D. Katz, and A. Schafer, *Phys. Rev. D* **86**, 071502 (2012).
- [11] G. S. Bali, F. Bruckmann, G. Endrodi, F. Gruber, and A. Schaefer, *J. High Energy Phys.* **04**, 130 (2013).
- [12] D. E. Kharzeev and D. T. Son, *Phys. Rev. Lett.* **106**, 062301 (2011).
- [13] Anping Huang et. al., *Phys. Rev. C* **107**, 034901 (2023).
- [14] S. Gupta, *Phys. Lett. B* **597**, 57 (2004).
- [15] G. Coccia *et al.*, *Nucl. Phys. A* **982**, 189 (2019).
- [16] M. A. Andreichikov *et al.*, *Phys.Rev. D* **87**, 094029 (2013).
- [17] C. S. Machado, S. I. Finazzo, R. D. Matheus, J. Noronha, *Phys. Rev. D* **89**, 074027 (2014).
- [18] J.P. Carlomagno *et al.*, *Phys. Rev. D* **106**, 094035 (2022).
- [19] Tetsuya Yoshida, Kei Suzuki, *Phys. Rev. D* **94**, 074043 (2016).
- [20] A. Broderick, M. Prakash, and J. M. Lattimer, *Astrophys. J.* **537**, 351 (2000).
- [21] A. E. Broderick, M. Prakash, and J. M. Lattimer, *Phys. Lett. B* **531**, 167 (2002).
- [22] M. Sinha, B. Mukhopadhyay, and A. Sedrakian, *Nucl. Phys. A* **898**, 43 (2013).
- [23] A. Rabhi, P. K. Panda, and C. Providencia, *Phys. Rev. C* **84**, 035803 (2011).
- [24] D.P. Menezes, M. Benghi Pinto, S. S. Avancini, A. P. Martinez, and C. Providencia, *Phys. Rev. C* **79**, 035807 (2009).
- [25] Joao Moreira, Pedro Costa and Tulio E. Restrepo, *Eur. Phys. J A* **57**, 123 (2021).
- [26] Yuan Wang and Xin-Jian Wen, *Phys. Rev. D* **105**, 074034 (2022).
- [27] P. Yue and H. Shen, *Phys. Rev. C* **77**, 045804 (2008).
- [28] V. Dexheimer, R. Negreiros, and S. Schramm, *Eur. Phys. J. A* **48**, 189 (2012).
- [29] Manisha Kumari and Arvind Kumar *Nucl. Phys. A* **1022**, 122442 (2022).



- [30] Nisha Chahal, Suneel Dutt and Arvind Kumar, Phys. Rev. C **107**, 045203 (2023).
- [31] P. C. Chu *et al.*, Phys. Lett. B **778**, 447 (2018).
- [32] D. P. Menezes, M. Benghi Pinto, S. S. Avancini, and C. Providencia, Phys. Rev. C **80**, 065805 (2009).
- [33] A. Haber, F. Preis, and A. Schmitt, Phys. Rev. D **90**, 125036 (2014)
- [34] Arghya Mukherjee, Snigdha Ghosh, Mahatsab Mandal, Sourav Sarkar and Pradip Roy, Phys. Rev. D **98**, 056024 (2018).
- [35] R. M. Aguirre and A. L. De Paoli, Eur. Phys. Jour. A **52**, 343 (2016).
- [36] R. M. Aguirre, Phys. Rev. C **100**, 065203 (2019).
- [37] Danning Li, Mei Huang, Yi Yange and Pei-Hung Yuan, Journal of High Energy Physics **02**, 30 (2017).
- [38] Zhen Fang, Phys. Lett. B **758**, 1 (2016).
- [39] Amruta Mishra and Arindam Mazumdar, Phys. Rev. C **79**, 024908 (2009).
- [40] Arvind Kumar and Amruta Mishra, Phys. Rev. C **81**, 065204 (2010).
- [41] P. Papazoglou, D. Zschesche, S. Schramm, J. Schaffner-Bielich, H. Stöcker, and W. Greiner, Phys. Rev. C **59**, 411 (1999).
- [42] Arvind Kumar and Amruta Mishra, Eur. Phys. J. A **47**, 164 (2011).
- [43] D. Pathak and A. Mishra, Adv. High Energy Phys. **2015**, 697514 (2015).
- [44] D. Pathak and A. Mishra, Phys. Rev. C **91**, 045206 (2015).
- [45] D. Pathak and A. Mishra, Int. J. Mod. Phys. E **23**, 1450073 (2014).
- [46] A. Mishra and D. Pathak, Phys. Rev. C **90**, 025201 (2014).
- [47] P. Sushruth Reddy, C. S. Amal Jahan, Nikhil Dhale, Amruta Mishra and Juergen Schaffner-Bielich, Phys. Rev. C **9**, 065208 (2018).
- [48] N. Dhale, S. Reddy P., A. Jahan C. S., A. Mishra, Phys. Rev. C **98**, 015202 (2018).
- [49] Amal Jahan CS, Nikhil Dhale, Sushruth Reddy P, Shivam Kesarwani, Amruta Mishra, Phys. Rev. C **98**, 065202 (2018).
- [50] A. Mishra , A. Jahan CS , S. Kesarwani , H. Raval , S. Kumar, and J. Meena , Eur. Phys. J. A **55**, 99 (2019).
- [51] Amal Jahan C.S., Shivam Kesarwani, Sushruth Reddy P., Nikhil Dhale, and Amruta Mishra, arXiv:1807.07572 (nucl-th).
- [52] Rajesh Kumar and Arvind Kumar, Phys. Rev. C **101**, 015202 (2020).

- [53] Rajesh Kumar, Rahul Chhabra and Arvind Kumar, Eur. Phys. J A **56**, 278 (2020).
- [54] A. Mishra, P. Parui, A. Kumar, and S. De, arXiv:1811.04622.
- [55] P. Parui, S. De, A. Kumar, and A. Mishra, arXiv:2104.05471.
- [56] Amruta Mishra and S. P. Misra, Int. Jour. Mod. Phys. E **30**, 2150064 (2021).
- [57] Amruta Mishra, S.P. Misra, Phys. Rev. C **102**, 045204 (2020).
- [58] Amruta Mishra, S.P. Misra, Int. Jour. Mod. Phys. E **31** 06, 2250060 (2022).
- [59] Pallabi Parui and Amruta Mishra, arXiv:2209.02455.
- [60] Ankit Kumar and Amruta Mishra, arXiv:2208.14962.
- [61] Sourodeep De, Pallabi Parui and Amruta Mishra, Int. J. Mod. Phys. E **31**, 2250106 (2022).
- [62] Amruta Mishra and S.P. Misra, Phys. Rev. D **107**, 074003 (2023).
- [63] Sourodeep De, Pallabi Parui, and Amruta Mishra, Phys. Rev. C **107**, 065204 (2023).
- [64] Pallabi Parui and Amruta Mishra, Phys. Rev. D **108**, 114025 (2023).
- [65] A Le Yaouanc et al, Phys. Lett. B **71**, 397 (1977).
- [66] Bengt Friman, Su Houng Lee and Taesoo Song, Phys. Lett. B **548**, 153 (2002).
- [67] S. P. Misra, Phys. Rev. D **18**, 1661 (1978).
- [68] S. P. Misra, Phys. Rev. D **18**, 1673 (1978).
- [69] Amruta Mishra, S. P. Misra and W. Greiner, Int. J. Mod. Phys. E **24**, 1550053 (2015).
- [70] Amruta Mishra and S. P. Misra, Phys. Rev. C **95**, 065206 (2017).
- [71] S. Weinberg, Phys. Rev. **166**, 1568 (1968).
- [72] S. Coleman, J. Wess, B. Zumino, Phys. Rev. **177**, 2239 (1969).
- [73] W. A. Bardeen and B. W. Lee, Phys. Rev. **177**, 2389 (1969).
- [74] D. Zschesche, A. Mishra, S. Schramm, H. Stöcker and W. Greiner, Phys. Rev. C **70**, 045202 (2004).
- [75] A. Mishra, K. Balazs, D. Zschesche, S. Schramm, H. Stöcker, and W. Greiner, Phys. Rev. C **69**, 024903 (2004).
- [76] J. Schechter, Phys. Rev. D **21**, 3393 (1980).
- [77] Erik K. Heide, Serge Rudaz and Paul J. Ellis, Nucl. Phys. A **571**, (2001) 713.
- [78] Amruta Mishra, Phys. Rev. C **91**, 035201 (2015).
- [79] J. F. Nieves, Phys. Rev. D **70**, 073001 (2004).
- [80] A. Mishra and S. Schramm, Phys. Rev. C **74**, 064904 (2006), A. Mishra, S. Schramm and W. Greiner, Phys. Rev. C **78**, 024901 (2008).

- [81] Amruta Mishra, Arvind Kumar, Sambuddha Sanyal, S. Schramm, Eur. Phys. J. A **41**, 205 (2009).
- [82] M.E. Peskin, Nucl. Phys. **B156**, 365 (1979).
- [83] G. Bhanot and M.E. Peskin, Nucl. Phys. **B156**, 391 (1979).
- [84] M.B.Voloshin, Nucl. Phys. B154 ,365 (1979).
- [85] Su Houng Lee and C.M. Ko, Phys. Rev. C **67**, 038202 (2003).
- [86] S. Cho, K. Hattori, S. H. Lee, K. Morita and S. Ozaki, Phys. Rev. Lett. **113**, 122301 (2014).
- [87] S. Cho, K. Hattori, S. H. Lee, K. Morita and S. Ozaki, Phys. Rev. D **91**, 045025 (2015).
- [88] K. Suzuki and S. H. Lee, Phys. Rev. C **96**, 035203 (2017).
- [89] J. Alford and M. Strickland, Phys. Rev. D **88**, 105017 (2013).
- [90] Amruta Mishra and S. P. Misra, Int. Jour. Mod. Phys. E **30**, 2150014 (2021).
- [91] S. Iwasaki, M. Oka, K. Suzuki, Eur. Phys. Jour. A **57**, 222 (2021).
- [92] L. Micu, Nucl. Phys. B **10**, 521 (1969).
- [93] A. Le Yaouanc, L. Oliver, O. Pene, J. C. Raynal, Phys. Rev. D **8**, 2223 (1973); *ibid*, Phys. Rev. D **9**, 1415 (1974); *ibid*, Phys. Rev. D **11**, 1272 (1975).
- [94] T. Barnes, F. E. Close, P. R. Page and E. S. Swanson, Phys. Rev. D **55**, 4157 (1997).
- [95] A. Chodos, R. L. Jaffe, K. Johnson and C. B. Thorn, Phys. Rev. D **10**, 2599 (1974).
- [96] Amruta Mishra, Ankit Kumar and S. P. Misra, Int. Jour. Mod. Phys. E **32**, 2350048 (2023).
- [97] Amruta Mishra and S. P. Misra, Eur. Phys. Jour. A **57**, 98 (2021).
- [98] A. Ilner, D. Cabrera, C. Markert and E. Bratkovskaya, Phys. Rev. C **95**, 014903 (2017).
- [99] A. Ilner, J. Blair, D. Cabrera, C. Markert and E. Bratkovskaya, Phys. Rev. C **99**, 024914 (2019).
- [100] A. Ilner, D. Cabrera, P. Srisawad and E. Bratkovskaya, Nucl. Phys. A **927**, 249 (2014).
- [101] K. Haglin, Nucl. Phys. A **584**, 719 (1995).
- [102] G. Q. Li, C. M . Ko and G. E. Brown, Nucl. Phys. A **611**, 539 (1996).